

# Very Low Mass Stars and Brown Dwarfs of the Young Open Cluster IC2391<sup>1</sup>

David Barrado y Navascués<sup>2,3</sup>,

*Max-Planck Institut für Astronomie. Königstuhl 17, Heidelberg, D-69117 Germany.*  
*barrado@pollux.ft.uam.es*

John R. Stauffer<sup>4</sup>

*Harvard-Smithsonian Center for Astrophysics, 60 Garden St., Cambridge, MA 02138, USA.*  
*jstauffer@cfa.harvard.edu*

César Briceño<sup>2</sup>

*Centro de Investigaciones de Astronomía (CIDA) Apartado Postal 264 Mérida, 5101-A*  
*Venezuela. briceno@cida.ve*

Brian Patten<sup>2</sup>

*Harvard-Smithsonian Center for Astrophysics, 60 Garden St., Cambridge, MA 02138, USA.*  
*bpatten@cfa.harvard.edu*

Nigel C. Hambly

*Institute for Astronomy, University of Edinburgh, Royal Observatory, Blackford Hill, Edinburgh*  
*EH9 3HJ, Scotland, UK. nch@roe.ac.uk*

and

Joseph D. Adams

*University of Massachusetts, Department of Physics and Astronomy, Amherst, MA 01003, USA.*  
*adams@pegasus.astro.umass.edu*

## ABSTRACT

We have identified a large sample of probable low mass members of the young open cluster IC2391 based on optical (VRIZ) and Infrared (JHK<sub>s</sub>) photometry. Our sample includes 50 probable members and 82 possible members, both very low mass stars and

---

<sup>2</sup>Visiting Astronomer, Cerro Tololo Inter-American Observatory. CTIO is operated by AURA, Inc. under contract to the National Science Foundation.

<sup>3</sup>Present address: Departamento de Física Teórica, C-XI. Universidad Autónoma de Madrid, Cantoblanco, E-28049 Madrid, Spain

<sup>4</sup>Present address: IPAC, California Institute of Technology, Pasadena, CA 91125, USA

brown dwarfs. We also provide accurate positions for these stars and brown dwarf candidates derived from red UK Schmidt plates measured using the microdensitometer SuperCOSMOS. Assuming an age of 53 Myr, we estimate that we have reached a mass of  $0.025 M_{\odot}$ , if the identified objects are indeed members of IC2391.

*Subject headings:* stars: low mass, brown dwarfs, open clusters and associations: IC2391

## 1. Introduction

IC2391 is one of the youngest and nearest open clusters. The *Hipparcos* distance modulus for the cluster is  $(m-M)_o \sim 5.82$ . As a compromise between various determinations of the distance modulus and *Hipparcos* parallaxes (Becker & Fenkart 1971; Lyngå 1987; van Leeuwen 1999; Robichon et al. 1999), we adopt  $(m-M)_0 = 5.95 \pm 0.1$ , corresponding to a distance of 155 pc. The mean reddening towards the cluster is small,  $E(B-V) = 0.06$  (Patten & Simon 1996). Prior to our lithium depletion age determination, the most commonly quoted age estimate for IC2391 was  $\sim 35$  Myr (Mermilliod 1981). In Barrado y Navascués, Stauffer & Patten (1999) we derived a new age estimate of  $53 \pm 5$  Myr.

Because of its proximity and youth, IC2391 has been the target of a number of recent studies. Rotational velocities, lithium abundances and  $H\alpha$  data for G, K and early M dwarf members can be found in Stauffer et al. (1989, 1997). X-ray fluxes, rotational periods and low resolution spectra for another set of probable cluster members are provided by Patten & Simon (1986) and Simon & Patten (1998). All these data support the conclusion that IC2391 is younger than the Alpha Per cluster ( $\sim 85$  Myr in the new lithium age scale, Stauffer et al. 1999; Barrado y Navascués, Stauffer, & Bouvier 1999; Stauffer & Barrado y Navascués 2000) but significantly older than 10 Myr (e.g., because the cluster contains no classical TTauri stars).

For an age of 35 Myr, we expected the lithium depletion boundary for IC2391 to be at  $I_C \leq 15.2$  (Baraffe 1998, private communication; Stauffer, Schultz, & Kirkpatrick 1998). The ROSAT images of the cluster only supplied candidate cluster members down to  $I_C \sim 15$ . No appropriate deep photographic plate sequences are available for a proper motion survey to the desired depth. We therefore obtained deep, multicolor photometric imaging of the cluster in order to produce a list of candidate cluster members. Because of the low galactic latitude of the cluster ( $b^{II} = -6.90$ ), our derived candidate list may be significantly contaminated by field stars. We therefore defer extensive discussion of these candidates until detailed spectroscopic follow-up is available.

In Section 2, we provide the details of our imaging program. The method we used to identify candidate cluster members is outlined in Section 3.

---

<sup>1</sup>Based on observations obtained at the Cerro Tololo Inter-American Observatory.

## 2. Observations and Data Reduction

### 2.1. The optical photometry and the initial selection of candidates

Our optical CCD photometric data (V,R<sub>C</sub>,I<sub>C</sub>,Z) were collected at the Cerro Tololo Inter-American observatory during four different observing runs: January 22, 1998, at the 0.9m (RI<sub>C</sub> filters); January 24–25, 1998, at the Blanco 4m telescope (RI<sub>C</sub> filters); April 4, 1998, at the 1.5m (RI<sub>C</sub> filters); and January 4–6, 1999, again with the 0.9m telescope (VI<sub>C</sub>Z filters). In the case of the CTIO 0.9m runs, we used the Tek 2048 #3 camera (0.43 arcsec/pix), yielding a field of view  $\sim 14$  arcmin on a side. For the CTIO 1.5m telescope, we used the CCD SITE 2048  $\times$  2048 imager at the f/7.5 focus, yielding an image scale of 0.44"/pix and a field of view of 14.8  $\times$  14.8 arcmin. For the Blanco telescope campaign, we used the Big Throughput Camera (BTC), a mosaic detector composed of four different 2048<sup>2</sup> pixel CCDs. Each CCD covers an area of 14.7  $\times$  14.7 arcmin, and the mosaic has a cross-shaped gap, 5.4 arcmin wide, between the CCDs. The total projected area on the sky of the BTC Mosaic is roughly 0.25 sq. deg., with a scale of 0.43 arcsec/pixel. The January 1998 and April 1998 runs were used to make sure we would be able to calibrate the BTC observations and to cover the gaps between the CCDs of the BTC mosaic. In total, we have covered an area close to 2.5 sq. deg. (2 sq. deg. with the BTC). Table 1 lists the coordinates of the center of each field, as well as the exposure times. Figure 1 shows the location of the observed area, together with our very low mass (VLM) stars and brown dwarf (BD) candidates (cross symbols).

The CCD images were bias-subtracted and flat-fielded using standard data reduction techniques and tools within IRAF<sup>5</sup>. The APPHOT package was used to extract instrumental magnitudes for the objects of interest in each CCD field.

### 2.2. The calibration of the data

All our 0.9m and 1.5m data were obtained under photometric conditions. Unfortunately, this was not the case for the CTIO 4m run (BTC data). Therefore, we used the first two sets of data from the 0.9m and 1.5m telescopes to calibrate the BTC data, corresponding to the (RI)<sub>C</sub> filters. This calibration included several steps. First, we extracted the instrumental magnitudes for all the CCDs using small apertures ( $\sim 2$  pixels, equivalent to  $\sim 0.9$  arcsec). Then, for each image, we derived an aperture correction ( $\sim 0.12$  mag). Using this method, we minimized the photometric errors, since we did not include flux from the nearby sky. Then, for the 0.9m and 1.5m data, we corrected for the airmass. We assumed the standard CTIO extinction coefficient (0.08 mag/airmass and 0.06 mag/airmass for the R<sub>C</sub> and I<sub>C</sub> filters, respectively). Standard stars from Landolt (1992) were observed in all cases, including the fields SA98, SA104, PG1047 and PG1323. They were

---

<sup>5</sup>IRAF is distributed by the National Optical Astronomy Observatories, which is operated by the Association of Universities for Research in Astronomy, Inc., under contract with the National Science Foundation.

used to calibrate the data into the Cousins system. Finally, the calibrated photometry from the 0.9m and 1.5m runs was compared with the instrumental magnitudes of the BTC campaign. This provided a zero point shift for each filter from which we computed calibrated magnitudes for the BTC survey. We did not find any significant color term between the three cameras/filter systems.

Table 1 lists the limiting magnitudes for each field in the  $R_C$  and  $I_C$  filters. The internal errors should be better than 0.15 magnitudes at the limiting magnitudes; and the photon statistical errors are  $\sim 0.01$  mag for  $R_C \sim 17$  and  $I_C \sim 16$  for the 0.9m and 1.5m data, and 0.01 for  $R_C \sim 19$  and  $I_C \sim 17.5$  for the BTC data. We have estimated the completeness limits from the histogram  $\text{Log } N_{\text{detections}}$  versus magnitude. These limits are defined by the magnitude where the histogram deviates from a straight line (see Wainscoat et al. 1992 and Santiago et al. 1996). In the case of the 0.9m and 1.5m data, they are  $R_C \sim 18.5$  and  $I_C \sim 18.0$  mag. For the BTC data, we have reached  $R_C \sim 20.5$  and  $I_C \sim 20$  mag.

In order to check the external accuracy of our optical data, we have carried out different comparisons. As stated before, we calibrated the BTC data using 2 different campaigns (0.9m and 1.5m telescopes) which took place immediately before and after that run. The comparison between these two runs gives dispersions of  $\sigma(R)=0.08$ ,  $\sigma(I)=0.07$  and  $\sigma(R-I)_C=0.01$ . The calibration of the BTC photometry has dispersions of 0.03 and 0.04 magnitudes for the  $R_C$  and  $I_C$  filters, respectively (rms scatter of the difference between the raw and calibrated magnitudes of the standard stars). Finally, the optical photometry for overlapping fields of the BTC survey agrees within 0.06 and 0.04 magnitudes (one sigma) for the  $R_C$  and  $I_C$  filters, after the calibration.

For the last observing run (January 1999, CTIO 0.9m), we used the  $VI_CZ$  filters and the photometry was calibrated independently. The V-band instrumental magnitudes were corrected for the effects of atmospheric extinction and were placed on the standard system (Johnson-Kron-Cousins) using observations of photometric standard stars (Landolt 1992) and previously determined  $(R-I)_C$  colors for our program objects. Because the  $I_C$  and  $Z$  CCD images were taken in consecutive pairs (i.e., at the same airmass) and because at that time there were no well-established standard stars for  $Z$  filter photometry in the literature, we did not perform an absolute calibration of the  $I_C$  and  $Z$  data. Instead, an  $(I-Z)_{CTIO}$  color index was calculated using just the  $I$  and  $Z$  instrumental magnitudes. As in Zapatero Osorio et al. (1999), we set  $I_C=Z$  for those standard stars observed with  $(R-I) \sim 0$  in order to determine a zero-point correction for our  $(I-Z)_{CTIO}$  color index.

The internal errors of our V-band photometry are estimated to range from  $\sim 0.02$  mag for  $V \sim 17$  to  $\sim 0.15$  mag for  $V \sim 21$ . The external errors on the  $V$  magnitudes may be larger since our typical program stars are much redder than any of the standard stars used to determine the transformation to the standard system. The uncertainties in the  $(I-Z)_{CTIO}$  color are estimated from the errors in the  $I_C$  and  $Z$  magnitudes as supplied by the PHOT routine in IRAF. They are computed as  $\Delta(Z-I)^2 = \Delta Z^2 + \Delta I^2$ . These should be on the order of 0.02 mag or less for the majority of the objects in our IC 2391 sample (for  $I_C \sim 17$  mag).

### 2.3. Infrared photometry

The infrared data were obtained by the 2MASS survey (Skrutskie et al. 1997) at the CTIO facility during November 21-25 and November 28-29, 1998 and processed at IPAC in January, 1999. All 2MASS scans used for this analysis were observed under photometric conditions. Based on photometric error and total sources detected with magnitude we estimate that these 2MASS data still reach  $\geq 0.99$  completeness and  $\text{SNR} \geq 10$  at  $J = 15.8$ ,  $H = 15.1$ , and  $Ks = 14.3$  despite any possible confusion noise in this field.

Both our optical data and the 2MASS survey have very accurate coordinates (see next subsection). Therefore, using the optical coordinates as input, we searched in the 2MASS catalog for a IR counterpart, using a 3 arcsec radii for this search, much larger than the errors in the coordinates.

### 2.4. Coordinates

To define astrometric solutions for the CCD frames we used secondary astrometric standards derived from United Kingdom Schmidt photographic plate material measured using the precision microdensitometer SuperCOSMOS (eg. Hambly et al. 1998). The global astrometric solution for the Schmidt plate was derived using the Tycho–ACT reference catalog (Urban, Corbin & Wycoff 1998), and includes correction for non-linear systematic effects caused by the mechanical deformation of the plates during exposure (eg. Irwin et al. 1998). We used the "short red" survey plate R6843 (epoch 1981.3, field number 165) for IC2391. These exposures, taken at low galactic latitudes, are far less crowded than the sky limited survey plates and reach  $R \sim 20$  (as opposed to  $R \sim 22$  for the deep survey plates). They are ideal for accurate astrometry of secondary standards as faint as  $R=20$  which overlaps with unsaturated objects on the CCD frames. The RMS residual per ACT star in the global astrometric plate solution was  $\sim 0.1$  arcsec in both coordinates; we estimate that there will be no systematic errors in the CCD astrometric solutions larger than this value. The positions of our IC2391 candidates are listed in Table 2.

## 3. Discussion

### 3.1. Initial selection of candidate members of IC2391

The initial selection of candidate members of IC2391 was carried out using the location of the detected stars on the  $I_C$  versus  $(R-I)_C$  color-magnitude diagram. Figure 2 displays the data obtained at the 4m CTIO/BTC telescope, where detections are shown as dots. An empirical Zero Age Main Sequence (ZAMS), based on data from Leggett (1992), is included as a solid line. The ZAMS is plotted for our assumed IC2391 distance modulus and a reddening of  $E(R-I)=0.007$  [David: is this  $E(R-I)$  compatible with the  $E(B-V)$  mentioned earlier in the text?] Completeness and limiting magnitudes are depicted as dashed lines. We selected all the detected objects in a wide

band well above the ZAMS. The lower envelope for the strip follows a 50 Myr isochrone (D’Antona & Mazzitelli 1997) and the upper envelope is displaced 0.75 mag brighter to include equal mass binaries. The boundaries of the strip were also adjusted to take into account the photometric errors and errors in the distance, age and the reddening. Hence, this band is wider than the 0.75 mag. Then, all candidates were visually inspected on the original images, in order to avoid the presence of false detections, and to verify the stellar-like shape of the detections and the lack of nearby bright stars or cosmic rays which could modify the photometry of the candidate. Since there is no clear separation between the field stars and the location of the cluster isochrone, we expect a strong contamination by spurious members. Specifically, those candidates located only slightly above the ZAMS should be considered with some caution, since they are well below the 50 Myr isochrone. In total, we have selected 206 candidate members, 94 from the BTC survey and another 112 from the 0.9m and 1.5m data. Figure 3 shows all our candidate members as circles. Solid circles indicate the position of the candidates whose membership has been confirmed spectroscopically, via radial velocity, spectral type and several spectroscopic features ( $H\alpha$ ,  $NaI8200\text{\AA}$ ). These results are discussed in Barrado y Navascués, Stauffer, & Patten (1999), where we provide a lithium depletion boundary (see Barrado y Navascués, Stauffer & Bouvier 1999) age for the cluster ( $53\pm 5$  Myr). Figure 3 also displays the position of a 50 Myr isochrone (short-dashed line), adapted from D’Antona & Mazzitelli (1997). Based on our spectroscopically confirmed members and on Simon & Patten (1996) data, we have created an empirical IC2391 isochrone, shown as a long-dashed line.

Table 2 lists the positions, optical and infrared photometry, the separation between the optical detection and the IR source and the identification with stars from the literature, for each candidate.

### 3.2. Color-Magnitude and Color-Color Diagrams of IC2391

The merger of our  $RI_C$  data with the 2MASS photometry, and the additional  $VI_CZ$  photometry collected in January 1999, allows us to create a large database of optical-infrared broadband photometry in 7 different filters. Therefore, we have been able to construct several color-magnitude and color-color diagrams. We have used these diagrams to estimate the membership status of each candidate.

Figure 4a depicts the  $[V,(V-I_C)]$  diagram. The empirical main sequence (MS) for young disk stars by Leggett (1992) is included as a solid line. This MS was built for M0-M9 dwarfs, in the ranges  $6.65 \leq M(I_C) \leq 14.67$ ,  $4.77 \leq M(K_{cit}) \leq 10.17$ ,  $0.75 \leq (R-I)_C \leq 2.30$ , and  $0.17 \leq (H-K) \leq 0.48$ . Note that our 2MASS data were taken in  $K_s$ . However, there are no important differences between the  $K_s$  and  $K_{cit}$  systems (see Persson et al 1998). For comparison purposes, the shift of the photometry corresponding to an interstellar absorption of  $A_v=2$  is plotted as an arrow. Proposed members of IC2391 from the literature (Patten and Simon 1996; Patten and Pavlovski 1999) appear as crosses. Figure 4b displays the  $I_C$  magnitudes against the  $(I_C-K_s)$  color, whereas Figure 4c shows the  $K_s$  magnitudes against the  $(J-K_s)$ . In all these figures, solid triangles represent initial candidate members whose membership has been rejected based on Figures 4 and 5 (probable

non-members), whereas open triangles show the possible non-members. Possible and probable members are represented by open and solid circles, respectively (see next subsection).

Several color-color diagrams can be found in Figure 5. Symbols are as in Figure 4. Panel a and b depict  $[(V-R_C), (R-I)_C]$ , and  $[(I_C-K_s), (R-I)_C]$ , respectively. It is clear from examination of these diagrams that our original sample included both stars that are plausible cluster members and objects that are instead very likely to be heavily reddened, background stars.

### 3.3. A final list of photometric candidate members

In order to remove the spurious members present in our candidate member list, we have used several color-color diagrams and color-magnitude diagrams. This selection was carried out in a hierarchical way, stressing the spectroscopic and IR data. The scheme we followed is described below:

1. A fraction of our candidates has intermediate resolution spectroscopy (Barrado y Navascués et al. 1999), which indicates whether they are probable members or non-members.
2. We have removed the objects having a large interstellar reddening (see Figure 4b,c and Figure 5b). They were classified as probable non-members.
3. Color-color diagrams were used to remove additional probable non-members (Figures 5a,b).
4. Objects fainter than  $I_C=17$  mag, and without IR data (they are too faint to be detected by the 2MASS survey) were classified as possible members, whereas stars brighter than this value, with no IR data (they should have been detected by 2MASS) are listed as possible non-members.
5. Objects bluer than the Leggett’s (1992) IR main-sequence appear in Table 2 as possible members.
6. Objects bluer than our empirical optical isochrone or at the upper (bright) edge of our CM diagram selection strip were also classified as possible members.
7. Finally, the objects that remain are considered to be bona fide members of the cluster (“probable members”).

As a summary, we have classified our initial IC2391 candidate members in four different categories:

- Probable members. Objects located in all CM and CC diagrams with positions which indicate membership. They are identified with the flag “*MEM*” in the last column of Table 2 (50 objects, including 16 having spectroscopy).

- Possible members (82 objects). They appear identified with the flag “*MEM?*” in Table 2.
- Possible non-members (10). (“*NM?*” flag).
- Probable non-members (64). All of them are flagged with “*NM*” in Table 2.

If we only consider our probable members, we have detected objects  $\sim 2$  magnitudes fainter than the previous surveys (Rolleston & Byrne 1997; Simon & Patten 1998; Patten & Pavlovsky 1999). Our faintest possible IC2391 member has  $I_C=20.9$ , which is 5 magnitudes fainter than the least massive candidate discovered to date. In total, we list 132 objects as probable or possible members of IC2391.

We have not computed the luminosity function (LF) and mass function (MF). Due to its low galactic latitude of the cluster ( $b^{II}=-6.90$ ), even when using the probable/possible member list, pollution by spurious members is likely to be significant. Visual inspection of the  $I,(R-I)_C$  color-magnitude diagram (Figure 3) reveals two important characteristics: the relative high number of candidate members with  $I_C$  in the range 19.5–20.9, and the apparent gap just before this clustering occurs. Only additional photometry or spectroscopy would allow us to establish if these faint candidates are real. However, we expect a strong contamination by field stars in this range. If most of these objects are, indeed, not members, the gap would be illusory and the low number of candidate members below  $I_C=18$  could be a consequence of our completeness limit (dotted line in Figure 3). The question is still open, until a follow-up spectroscopic study is carried out.

### 3.4. The contamination by field stars

In a deep optical survey of the Pleiades, Bouvier et al. (1998) estimated that the contamination due to field stars was 25%. This value has been confirmed by subsequent spectroscopic follow-up of the Pleiades candidates. Since IC2391 is closer to the Galactic Plane than the Pleiades ( $b^{II}=-6.90$  and  $b^{II}=-23.52$ , respectively), the contamination should be much stronger. In fact, Figure 2 of Bouvier et al. (1998) shows a clear discontinuity between field stars and the Pleiades population. This is not the case for IC2391, whose color-magnitude diagram (Figure 3) depicts a smooth transition between the field and the locus of the main sequence of the cluster, indicating that contamination by spurious members should be stronger than in the case of the Pleiades. To estimate the degree of contamination by field stars, we have constructed histograms of the number of stars per magnitude bin at various  $(R-I)_C$  color intervals. In Figure 6 we show the histogram for the  $(R-I)_C=1.9-2.0$  range, representative of the distribution of stars down to approximately the completeness limit of the BTC data. The locus of the cluster is indicated. Similar diagrams for adjoining color ranges provide analogous results. The last bin before the cluster contains 3 stars, whereas the brightest bin, well above the main sequence for equal mass binary cluster stars (0.75 brighter than the single star MS), has 5 stars. The bins in between have 17 stars. Assuming an average contamination of 4 stars per bin, the pollution rate would be  $\sim 50\%$  for



the initial list of IC2391 candidates (the  $RI_C$  survey). Our optical and infrared color-color and color-magnitude diagrams have allowed us to remove about 33% of the candidates from the initial 206 objects. Therefore, we estimate that objects cataloged as members in Table 2 (probable and possible members) still have a  $\sim 25\%$  or greater probability of being spurious.

The faintest objects, lacking VZJHK data, may be more strongly polluted by field stars.

### 3.5. Brown Dwarfs in the Cluster

Based on the position of the lithium depletion boundary in members of IC2391, Barrado y Navascués, Stauffer, & Patten (1999) have recently determined an age for the cluster of  $53 \pm 5$  Myr. For this age, the border between the stellar and substellar regimes would be at  $M(I_C) = 11.06$  (Baraffe 2000, private communication). Taking into account the IC2391 distance and reddening, this leads to  $I_C = 17.03$ . Therefore, all our IC2391 candidates fainter than that value should be brown dwarfs if they indeed belong to the cluster. Our list of final candidates contains ten objects which have been cataloged as probable and possible members based on both optical and infrared data and which have  $I_C$  in the range 17.06–17.62. Using the Baraffe (2000) models, their mass range is 0.070–0.055  $M_\odot$ . Actually, two of these objects (CTIO-061 and CTIO-113) have been observed using low S/N, intermediate resolution spectroscopy (Barrado y Navascués, Stauffer, & Patten 1999). Several spectral characteristics, such as  $H\alpha$  and  $\text{NaI}8200\text{\AA}$  equivalent widths, spectral type, rough radial velocities, indicate that they are real members of the cluster and, therefore, brown dwarfs.

Another 50 objects in Table 2 are fainter than than the  $I_C$  magnitude of the stellar/substellar limit and lack infrared data. All of them are listed as possible members in Table 2, with magnitudes down to  $I_C = 20.9$ ,  $M(I_C) = 14.93$ , and  $M \geq 0.025 M_\odot$ .

### 3.6. Comparison with previous surveys and other clusters

A comparison between our final candidate members (circles) and previous surveys (triangles) of IC2391 is shown in Figure 7a. Probable candidate members are displayed with solid circles, whereas open circles represent objects which do not have infrared counterparts (normally, because they are too faint to be detected by 2MASS). The stars from Simon & Patten (1996) are shown as solid triangle, and the objects from Patten & Pavlovsky (1999) appear as open triangles. Clearly, all these samples merge smoothly, describing a good cluster isochrone. Most of our probable candidate members are above the empirical isochrone, which was obtained based on confirmed members of the cluster (Figure 3). In fact, they are located in a wide band, slightly larger than  $\sim 0.75$  mag (the maximum shift due to binarity).

We have compared our optical data of IC2391 candidates with data from two other very well

known clusters. Figure 7b contains photometry from the Pleiades (asterisks), alpha Per (plus symbols) and IC2391 (solid and open circles for probable and possible members). These open clusters have lithium ages of 125, 85 and 53 Myr, respectively (Stauffer, Schultz, & Kirkpatrick 1998; Stauffer et al. 1999; Barrado y Navascués, Stauffer, & Patten 1999). The large width of the IC2391 main sequence, which includes probable and possible members, can be appreciated. However, this scatter is greatly reduced if we only take into account probable members. Then, the scatter is similar to the value present in the other two clusters. This is consistent with our previous estimate of the contamination for the possible members which are located at the blue side of our empirical IC2391 isochrone. Only further spectroscopy (or, eventually, proper motions) will allow us to verify the membership status of these objects. The comparison between the MS lower envelopes of these two clusters with the lower MS of IC2391 probable members suggests that, indeed, IC2391 is slightly younger than Alpha Per, and that both of them are considerably younger than the Pleiades.

#### 4. Summary

Using optical and infrared data, and based on the location on CM and CC diagrams, we have identified a large sample of very low mass stars and brown dwarf candidates of the young cluster IC2391. Accurate coordinates, derived from the SuperCOSMOS microdensitometer, are provided for all of them. We have established a total of 50 probable cluster members, based on their position in the cluster loci in all CC and CM diagrams. Another 82 objects have been cataloged by us as possible members. We have identified two candidate sub-stellar IC2391 members for which we have a full set of multicolor photometry, and whose location in all the CM and CC diagrams supports cluster membership. We have an additional 50 candidate substellar mass members in IC2391, but because we have less or poorer data for these objects we expect that many of them will instead be low mass field stars.

DBN thanks the “*Instituto Astrofísico de Canarias*” (Spain) and the “*Deutsche Forschungsgemeinschaft*” (Germany) for their fellowship. JRS acknowledges support from NASA Grant NAGW-2698 and 3690. This work has been partially supported by Spanish “*Plan Nacional del Espacio*”, under grant ESP98–1339-CO2. This publication makes use of data products from the Two Micron All Sky Survey, which is a joint project of the University of Massachusetts and the Infrared Processing and Analysis Center, funded by the National Aeronautics and Space Administration and the National Science Foundation.

## REFERENCES

- Barrado y Navascués D., Stauffer J. R., Bouvier, J. 1999 *Ap&SS* 263, 239
- Barrado y Navascués D., Stauffer J.R., Patten, B.M., 1999, *ApJ Letters* 522, L56
- Becker W., & Fenkart R. 1971, *A&AS* 4, 241
- Bouvier J., Stauffer J.R., Martín, E.L., Barrado y Navascués, D., Wallace B., Béjar, V., 1998, *A&A* 336, 490
- D’Antona F., & Mazzitelli I. 1997, in “Cool Stars in Clusters and Associations”, ed. R. Pallavicini & G. Micela, *Mem. Soc. Astron. Italiana*, 68 (4), 807
- Hambly N.C., Miller L., MacGillivray H.T., Herd J.T., Cormack W.A., 1998, *MNRAS*, 298, 897
- Irwin M.J., Hawkins M.R.S., Hambly N.C., MacGillivray H.T., 1998, *Anglo–Australian Observatory Newsletter No. 85 (April 1998)*, 14
- Jeffries R.D., 2000, in “Stellar Clusters and Associations: Convection, Rotation, and Dynamos”. R. Pallavicini, G. Micela and S. Sciortino (eds.) *ASP Conf. Series* 198, 245
- Landolt A., 1992, *AJ* 104, 340
- Leggett S., 1992 *ApJ SS* 82, 351
- Lyngå G. 1987, *Catalog of Open Cluster Data (5th Ed., Lund: Lund Observatory)*
- Mermilliod J.-C. 1981, *A&A* 97, 235
- Patten B. M., & Simon T. 1996, *ApJSS* 106, 489
- Patten B. M., & Pavlovski C. M. 1999, *PASP* 111, 210
- Persson S.E., Murphy D.C., Krzeminski W., Roth M., Rieke M.J., 1998, *AJ* 116, 2475
- Prosser C.F., 1992, *AJ*, 103, 488
- Prosser C.F., 1994, *AJ*, 107, 1422
- Rolleston W.R.J., Byrne P.B., 1997 *A&AS* 126, 357
- Robichon N., Arenou F., Mermilliod J.-C., & Turon C. 1999, *A&A* 345, 471
- Santiago B.X., Gilmore G., Elson R.A.W., 1996, *MNRAS* 281, 871
- Skrutskie, M. F.; Schneider, S. E.; Stiening, R.; Strom, S. E.; Weinberg, M. D.; Beichman, C.; Chester, T.; Cutri, R.; Lonsdale, C.; Elias, J.; Elston, R.; Capps, R.; Carpenter, J.; Huchra, J.; Liebert, J.; Monet, D.; Price, S.; Seitzer, P. in “The Impact of Large Scale Near-IR Sky Surveys”, eds. F. Garzon et al., p. 25. Dordrecht: Kluwer Academic Publishing Company, 1997

- Simon T., Patten B.M., 1996, PASP 110, 283
- Stauffer J. R., Hartmann L.W., Jones B.J., & McNamara, B.R. 1989, ApJ 342, 285
- Stauffer J.R., Hartmann L.W., Prosser C.F., Randich S., Balachandran S., Patten B.M., Simon T., Giampapa M., ApJ 479, 776
- Stauffer J.R., Schultz G., Kirkpatrick J.D., 1998, ApJ Letters 449, L199
- Stauffer J.R., Barrado y Navascués D., Bouvier J., Morrison H.L., Harding P, Luhman K., Stanke T., McCaughrean M., Terndrup D.M., Allen L., Assouad P., 1999, ApJ 527, 219
- Stauffer J.R., Barrado y Navascués D., , 2000, in " 11th Cambridge Workshop on Cool Stars, Stellar Systems and the Sun", García-López, Rebolo, & Zapatero-Osorio, Eds. ASP Conf. Series, in press.
- Urban S.E., Corbin T.E., Wycoff G.L., 1998, AJ 115, 2161
- Ushomirsky G., Matzner C.D., Brown E.F., Bildsten L., Hilliard V.G., & Schroeder P.C. 1998, ApJ 497, 253
- van Leeuwen F., 1999, A&A Letters 341, 71
- Wainscoat R.J., Cohen M., Volk K., Walker H.J. Schwartz D.E., 1992, ApJ SS 83, 111
- Zapatero-Osorio M.R., Rebolo R., Martín, E.L., Hodgkin S.T., Cossburn M.R., Magazzù A., Steele I.A., Jameson R.F., 1999, A&AS 134, 537

FIGURE CAPTIONS

Fig. 1.— Positions of our candidate members of IC2391 (plus symbols). The brightest stars in the field are represented as four-pointed stars.

Fig. 2.— All the photometry extracted from the 4m CTIO/BTC survey. The solid line indicates the positions of a ZAMS, whereas the long-dashed lines show the location of the detection and completeness limits. The completeness limit of the BTC survey is indicated by a dotted line.

Fig. 3.— Initial selection of candidates of IC2391 (open circles) based on  $RI_C$  data. Confirmed members (Barrado y Navascués et al. 1999) are displayed as solid circles. The solid, long-dashed and short dashed lines indicate the positions of a ZAMS, an empirical IC2391 isochrone and a 50 Myr isochrone (D’Antona & Mazzitelli 1997).

Fig. 4.— Color-magnitude diagrams of IC2391. Solid circles represent the probable members of the cluster, whereas open circles correspond to possible members. Open and solid triangles are objects initially selected as members, whose membership has been rejected based of these CC and CM diagrams. Data from previous surveys appear as crosses. The solid line represents the locus of an empirical ZAMS (Leggett 1992), whereas the long-dashed line (panel a and b) corresponds to an empirical IC2391 isochrone. Panel a also includes a 50 Myr isochrone by D’Antona & Mazzitelli (1997).

Fig. 5.— Color-color diagrams of IC2391. Symbols as in Figure 4.

Fig. 6.— Number of stars with  $1.9 \leq (R-I)_C < 2.0$  against the  $I_C$  magnitude. The location of IC2391 is indicated.

Fig. 7.— Absolute  $I_C$  magnitude against the unreddened  $(R-I)_C$  color index. Comparison with data from previous searches of members of IC2391 (panel a) and members of other clusters (panel b). An empirical ZAMS and an empirical IC2391 isochrone are represented as solid and dashed lines, respectively. IC2391 data comes from this survey, Simon & Patten (1996) and Patten & Simon (1996). Alpha Per data were selected from Prosser (1992, 1994) and Stauffer et al. (1999). Finally, Pleiades data comes from Bouvier et al. (1998).

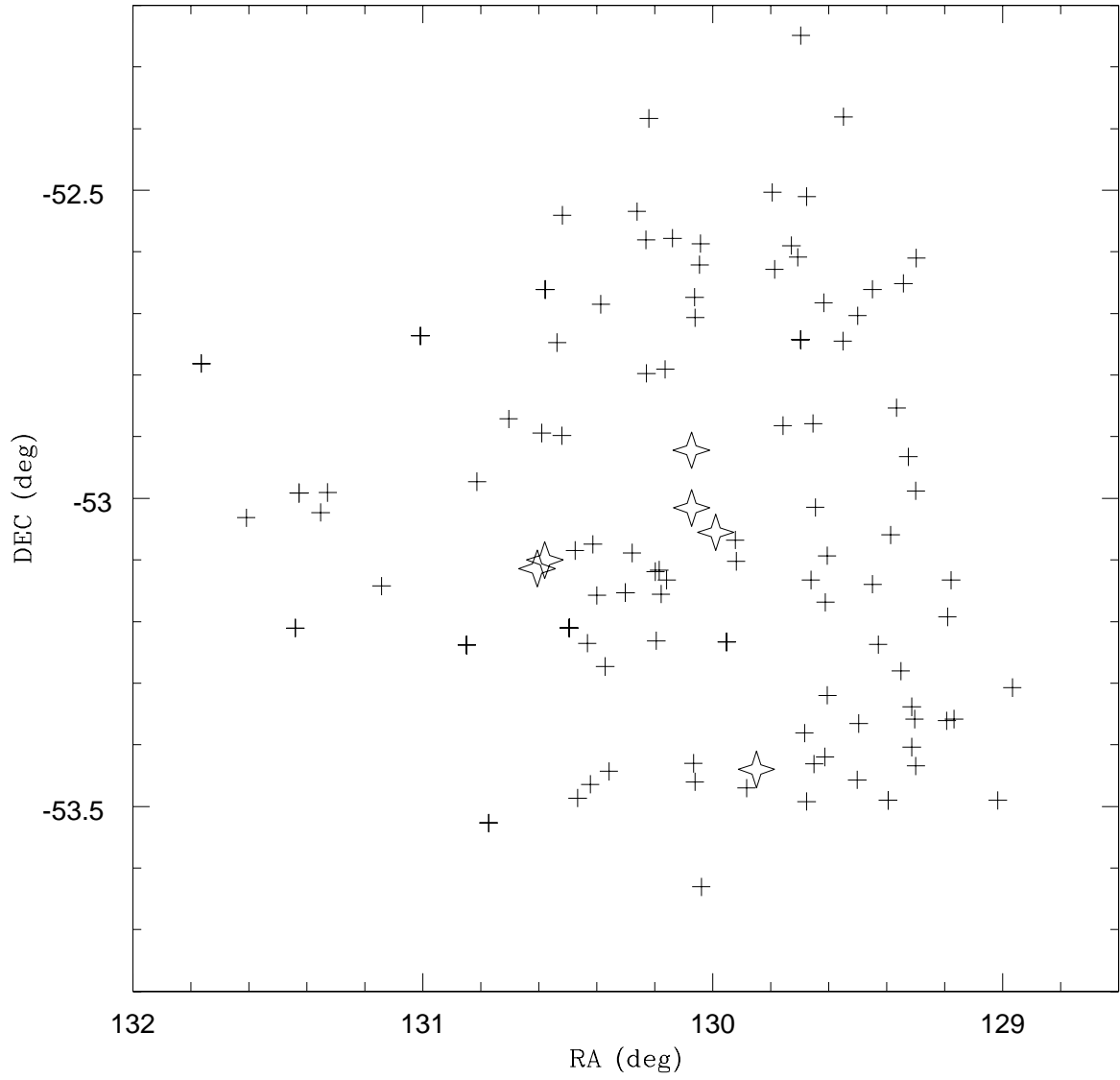


Fig. 1.— Positions of our candidate members of IC2391

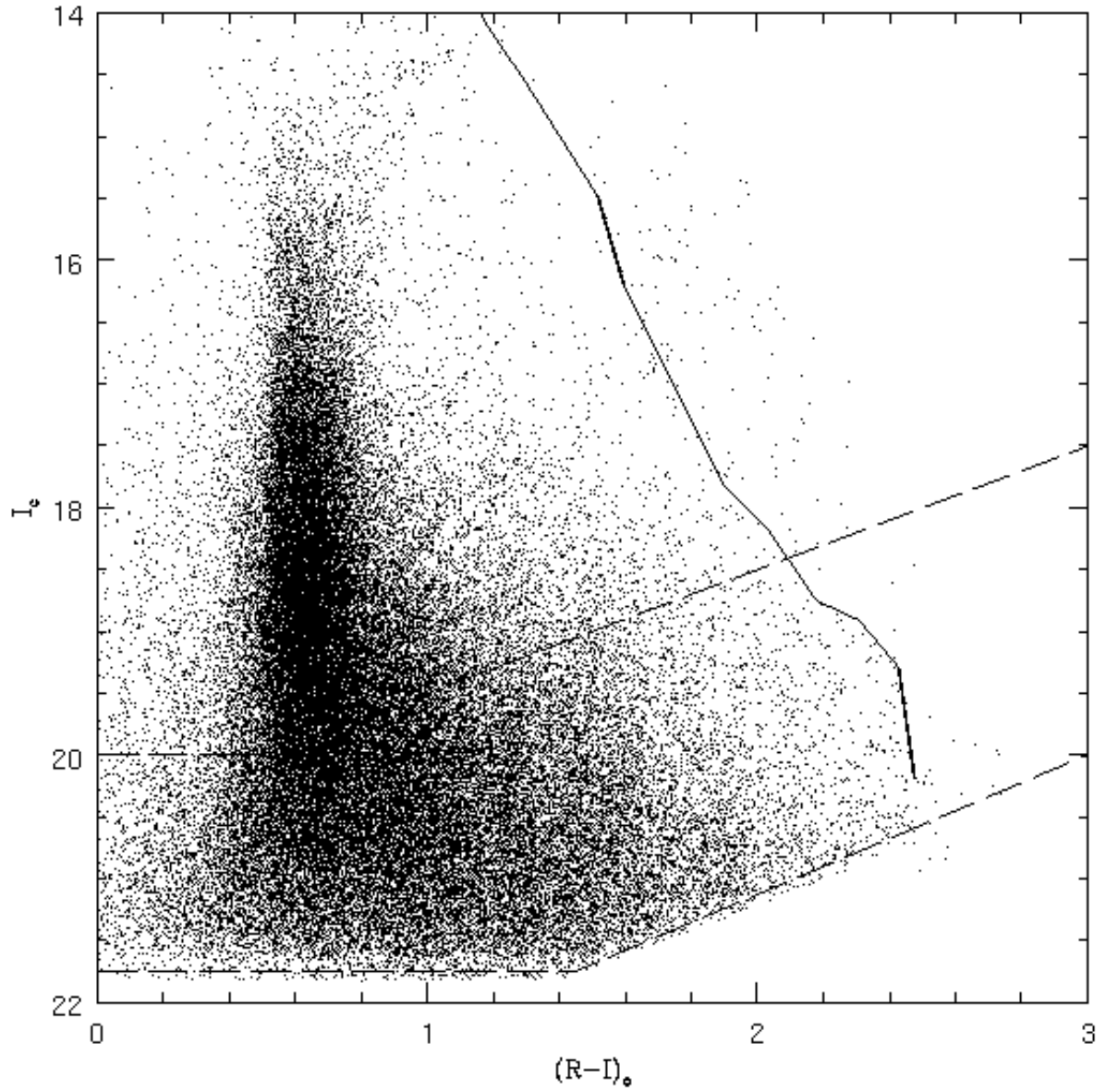


Fig. 2.— All the photometry extracted from the 4m CTIO/BTC survey. The solid line indicates the positions of a ZAMS, whereas the long-dashed lines show the location of the detection and completeness limits.

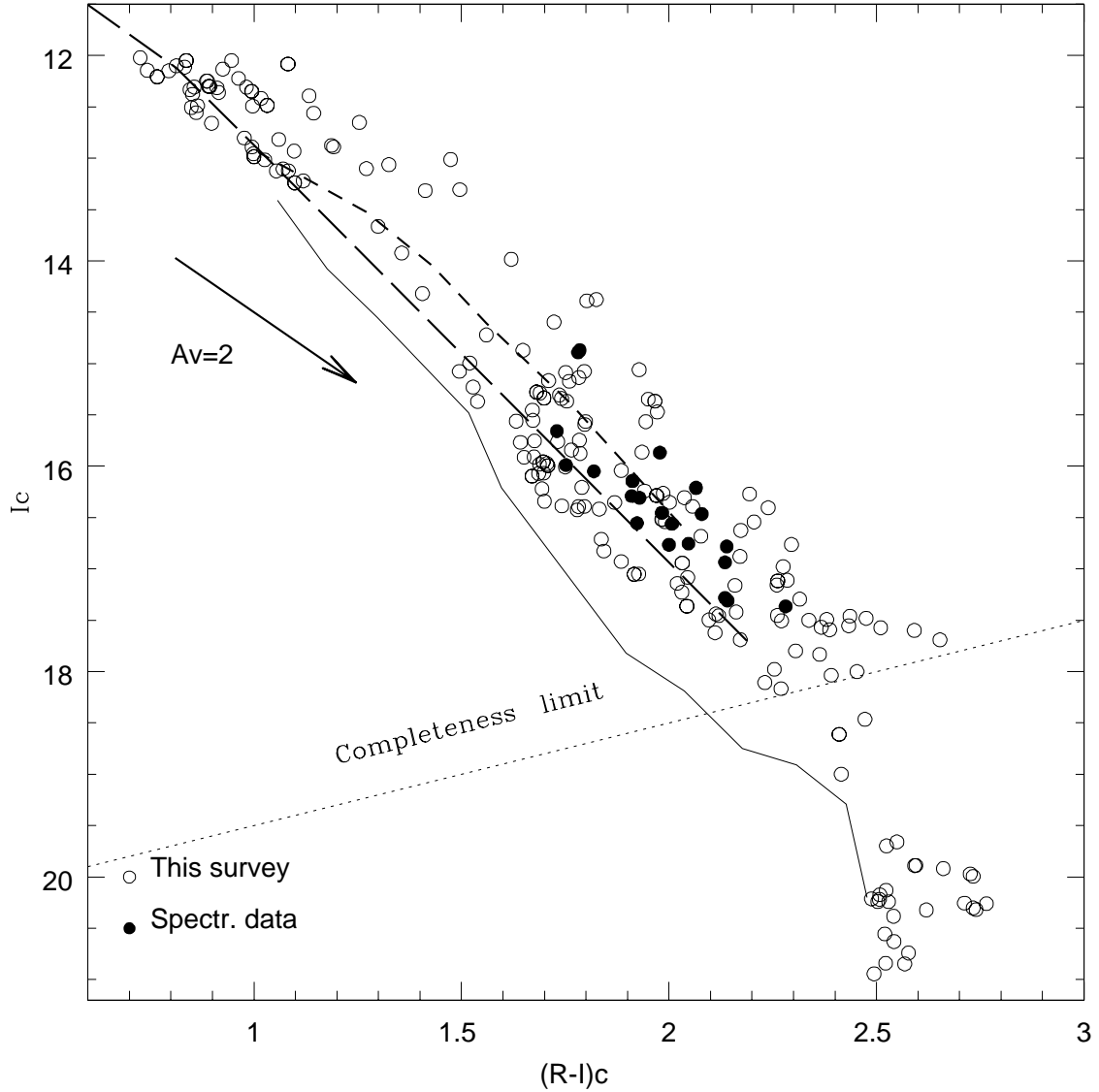


Fig. 3.— Initial selection of candidates of IC2391 (open circles). Spectroscopically confirmed members (Barrado y Navascués et al. 1999) are displayed as solid circles. The solid, long-dashed and short-dashed lines indicate the positions of a ZAMS, an empirical IC2391 isochrone and a 50 Myr isochrone (D’Antona & Mazzitelli 1997). The completeness limit of the BTC survey is indicated by a dotted line.



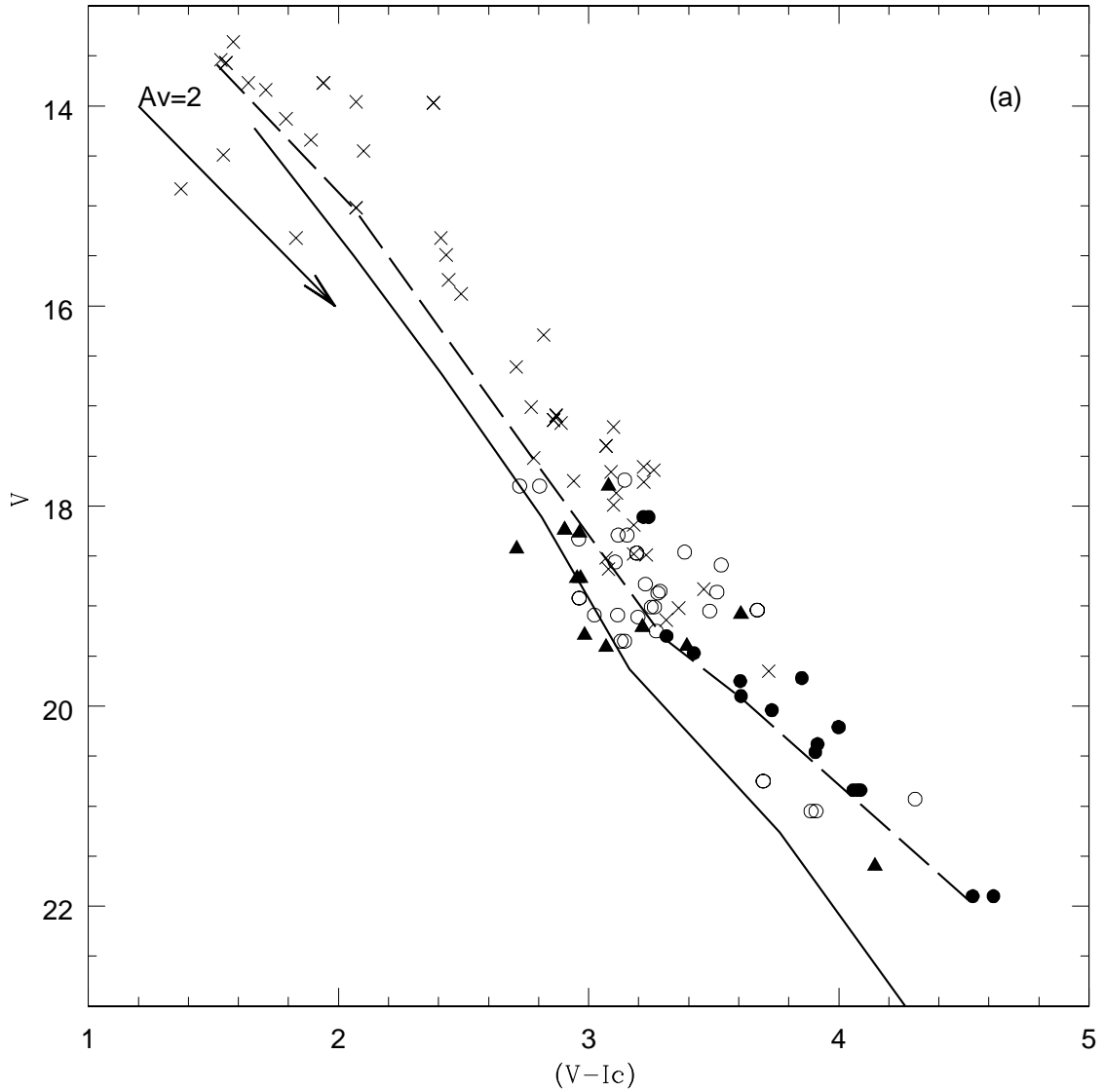


Fig. 4.— **a** Color-magnitude diagram of IC2391. Solid circles represent the probable members of the cluster, whereas open circles correspond to possible members. Open and solid triangles are objects initially selected as members, whose membership has been rejected based of these CC and CM diagrams. Data from previous surveys appear as crosses. The solid line represents the locus of an empirical Zero Age main-sequence, whereas the dashed line correspond to an empirical isochrone.

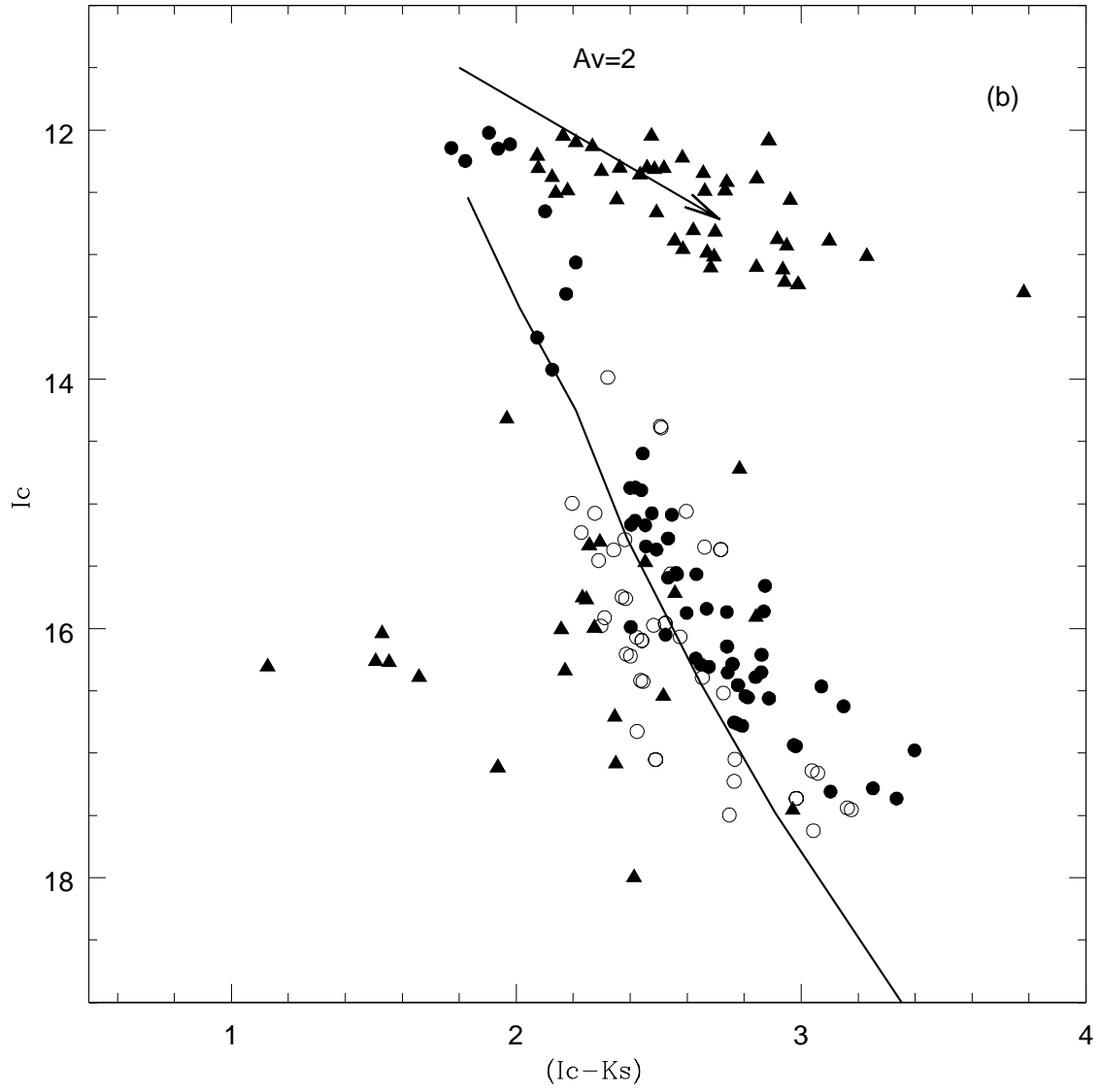


Fig. 4.— **b** Color-magnitude diagram of IC2391. Symbols as on Figure 4a.

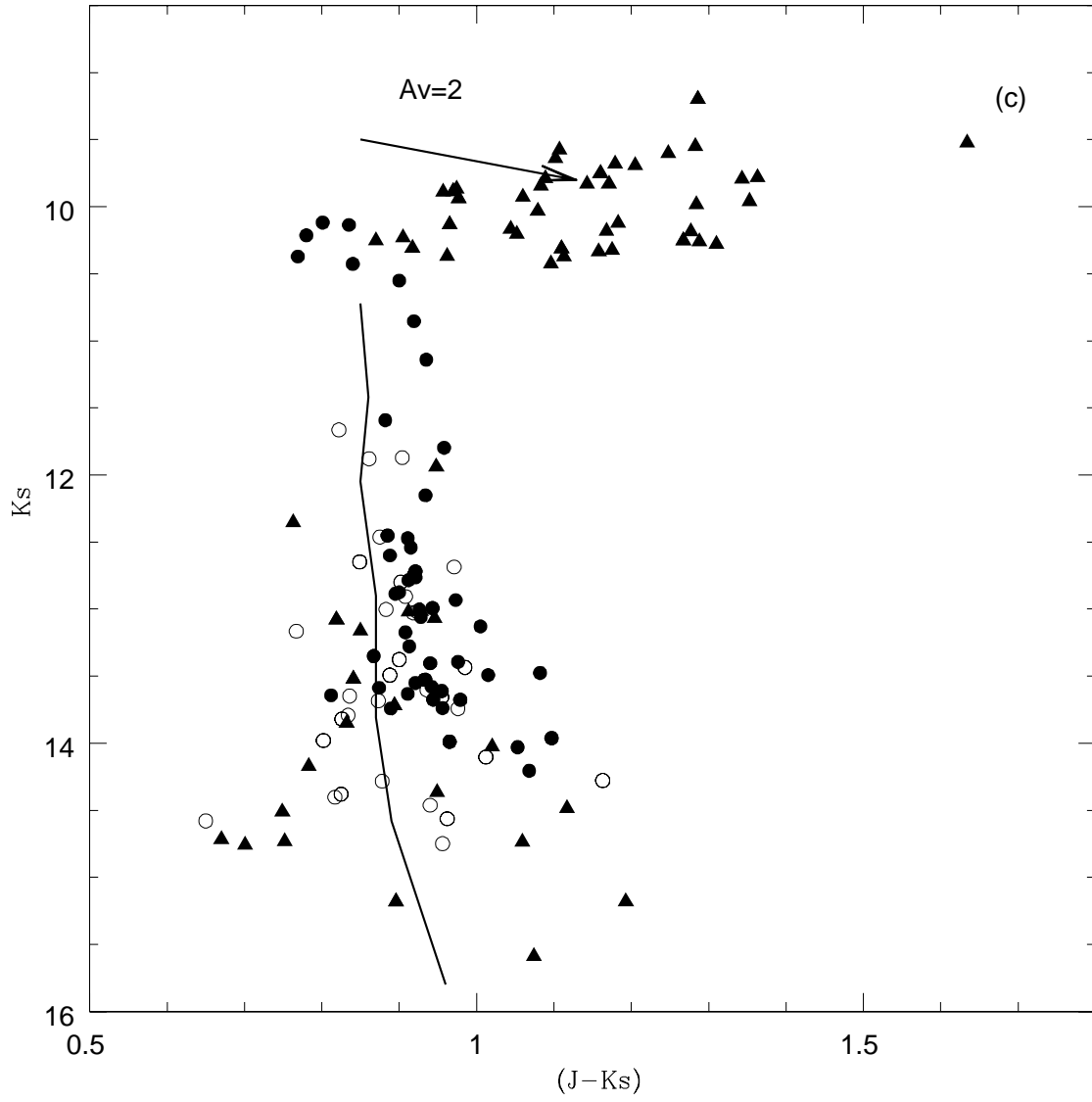


Fig. 4.— c Color-magnitude diagram of IC2391. Symbols as on Figure 4a.

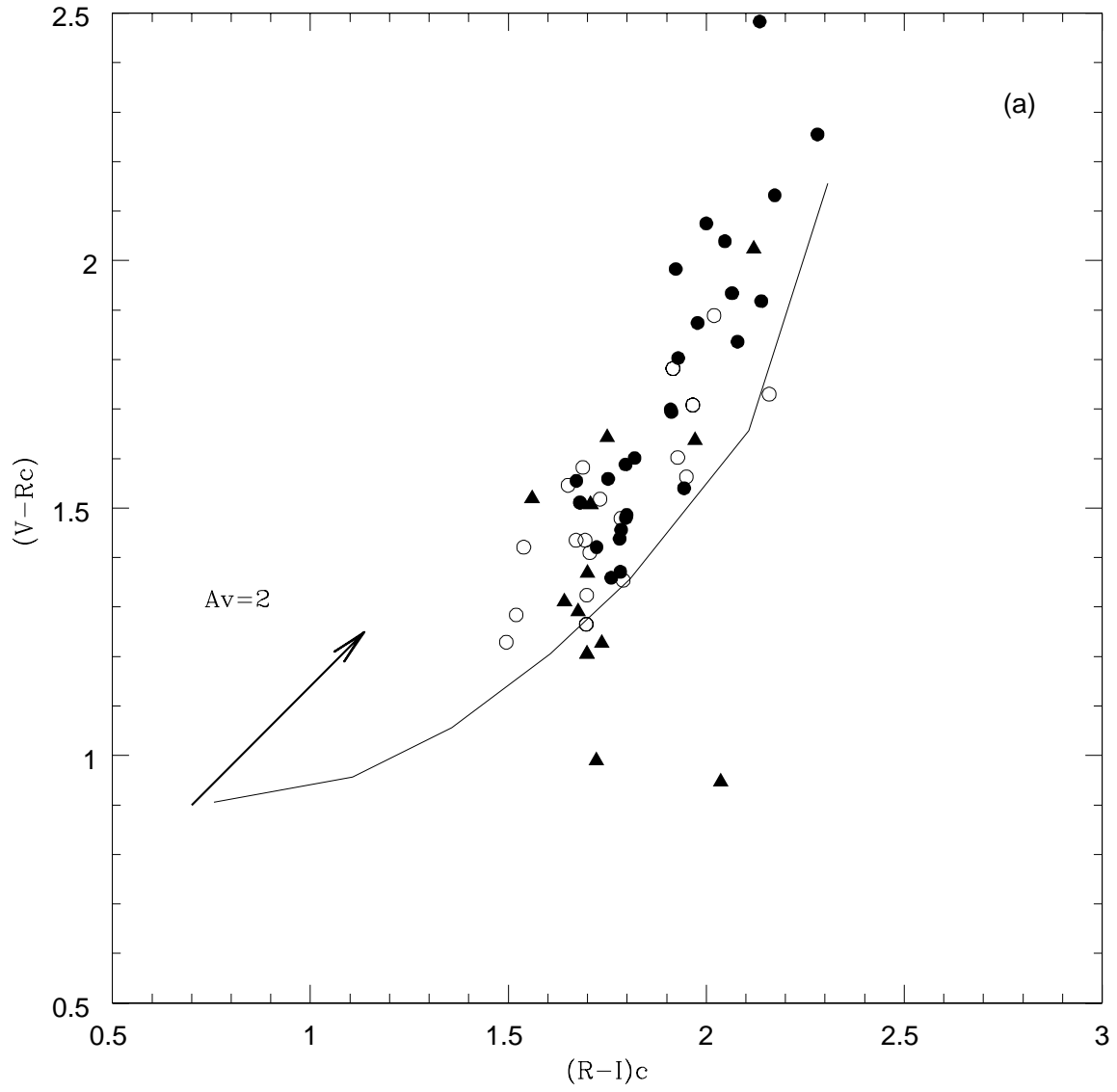


Fig. 5.— **a** Color-color diagram of IC2391. Symbols as on Figure 4.

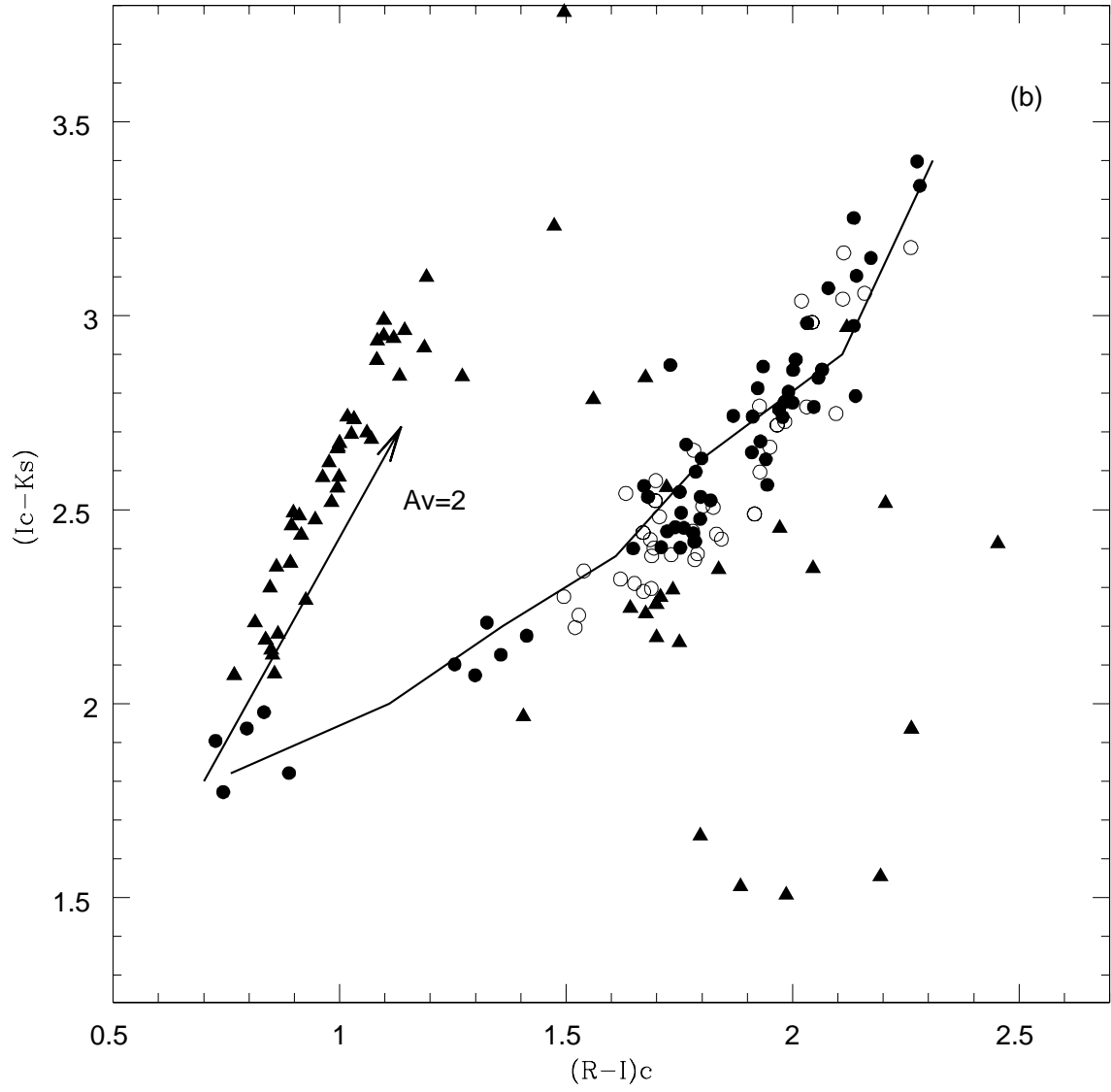


Fig. 5.— b Color-color diagram of IC2391. Symbols as on Figure 4.

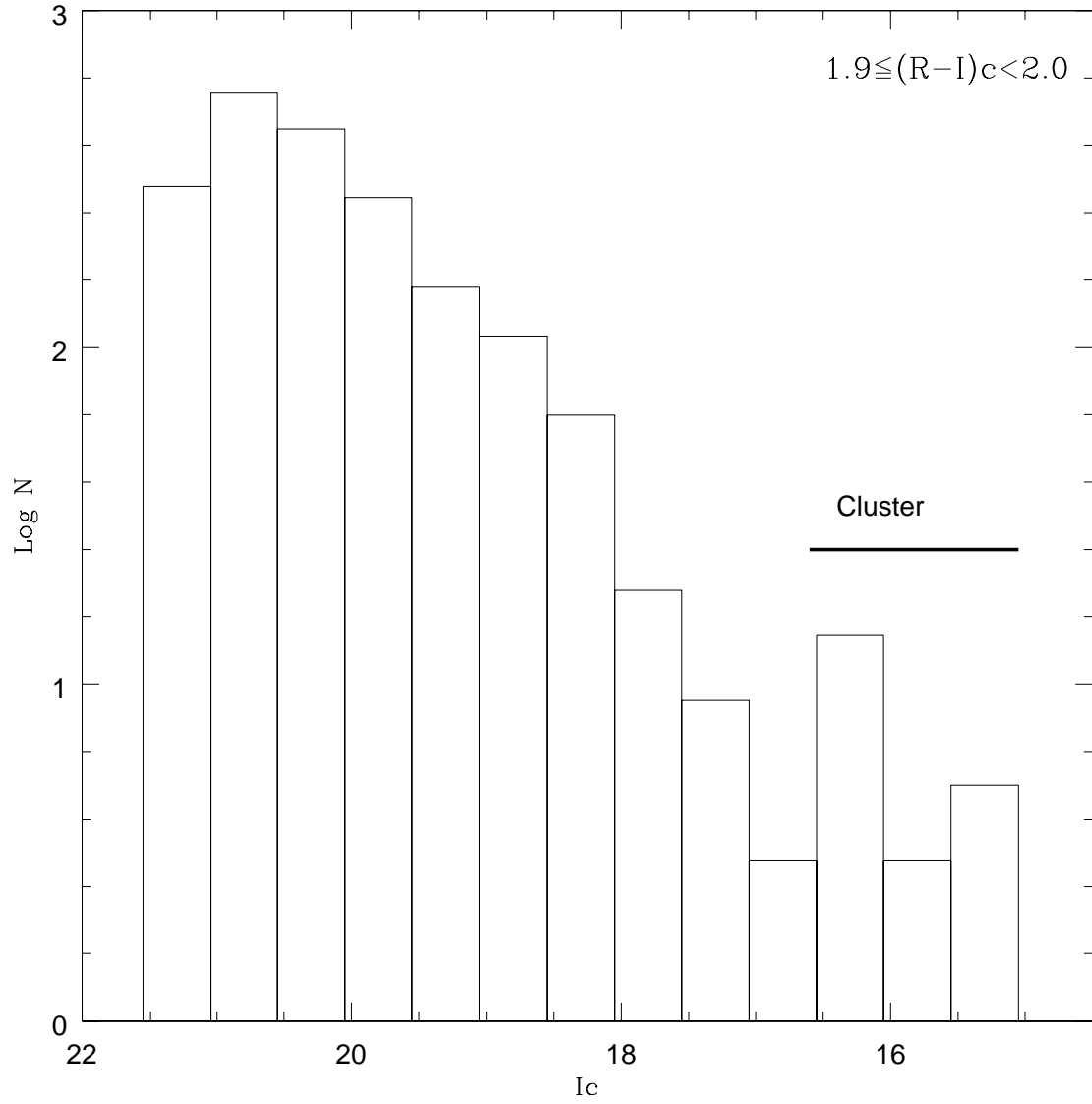


Fig. 6.— Frequency of stars with  $1.9 \leq (R-I)_c < 2.0$  against the  $I_c$  magnitude. The location of IC2391 is indicated.

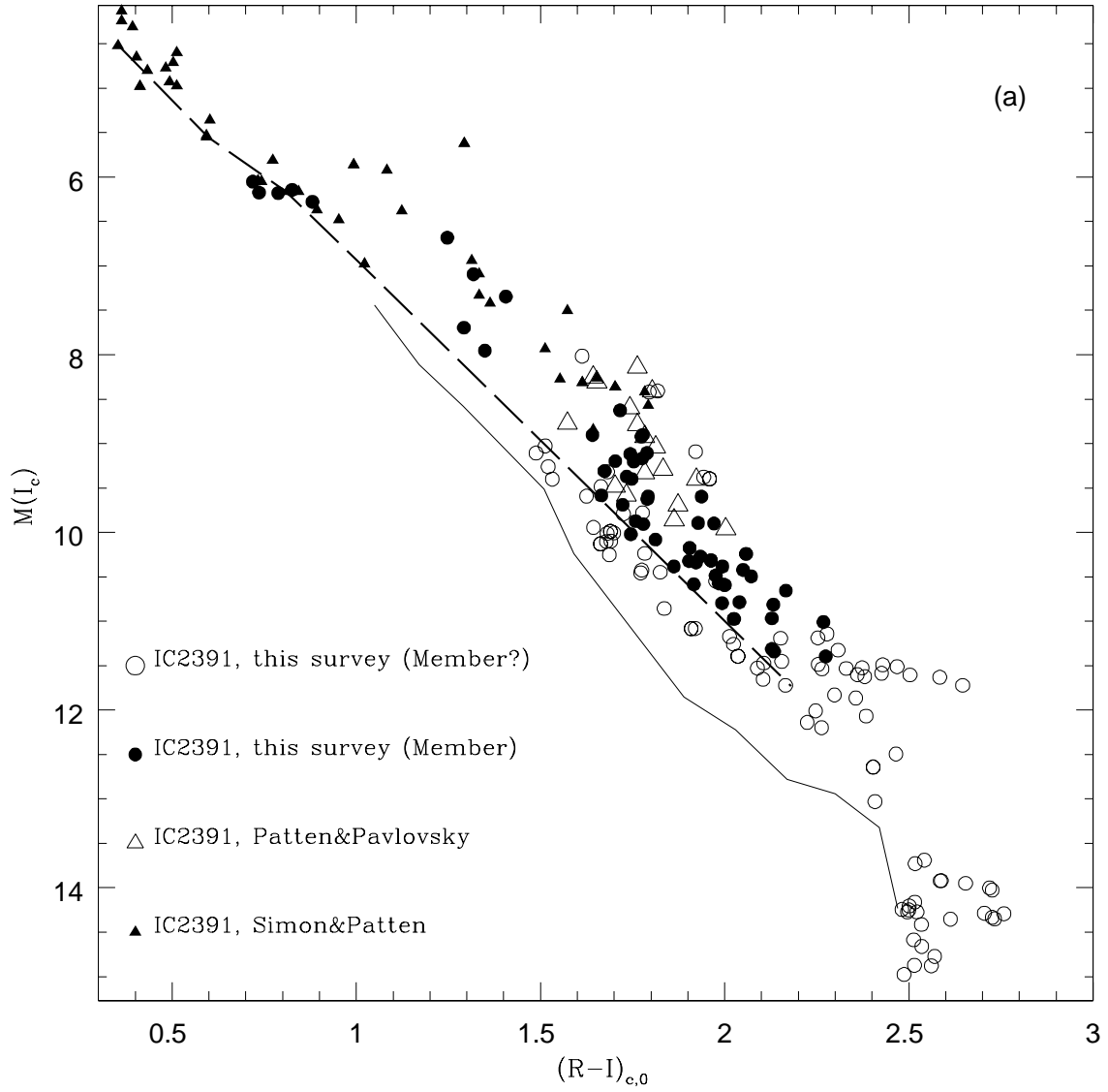


Fig. 7.— a Comparison with data from previous searches of members of IC2391.

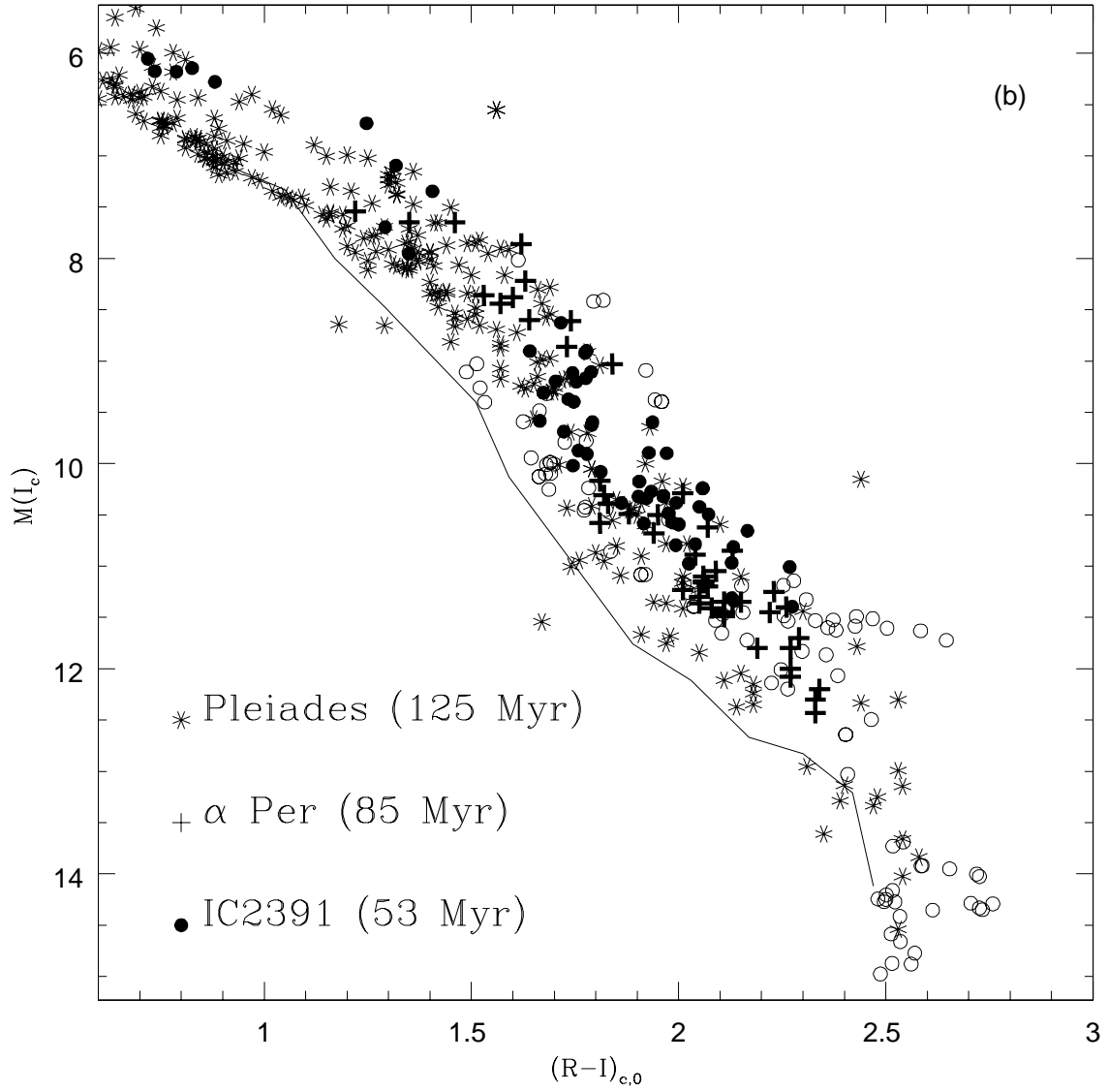


Fig. 7.— **b** Comparison between IC2301 candidate members (solid and open circles represent probable and possible members) and members of Alpha Per (crosses) and the Pleiades (asterisks)



Table 1: Field centers, exp. times and limiting magnitudes for the optical data

Field	RA	DEC	Exp. Time		Mag. limit	
	(2000.0)		$R_C$	$I_C$	$R_C$	$I_C$
	(h m s)	( $^{\circ}$ ' ")	(sec)	(sec)		
BTC #1	08:40:10	-53:20:01	2880	1200	23.1	21.7
BTC #1'	08:40:32	-53:19:58	1200	600	23.1	21.5
BTC #2	08:43:52	-53:26:25	1440	600	23.1	21.3
1.5m #2	08:43:52	-53:26:25	30	30	20.5	19.6
BTC #3	08:38:11	-52:46:44	960	960	22.8	19.4
1.5m #3	08:38:11	-52:46:44	30	30	20.5	19.6
BTC #3'	08:39:46	-52:31:03	1200	600	23.5	22.0
BTC #4	08:42:55	-52:46:59	600	1440	22.8	20.8
1.5m #4	08:42:55	-52:46:59	30	30	20.5	19.6
BTC #5	08:36:30	-53:20:00	1200	600	23.1	21.8
1.5m #5	08:36:30	-53:20:00	30	30	20.5	19.6
BTC #5'	08:37:04	-53:14:49	274	400	23.0	21.8
BTC #6	08:45:14	-52:56:50	1200	600	23.5	22.1
1.5m #6	08:45:14	-52:56:50	30	30	20.5	19.6

Table 2: IC2391 candidate members.

CTIO	ALPHA		DELTA		V	$I_C$	$(R-I)_C$	$(I-Z)$ <i>CTIO</i>	J	H	$K_s$	dist (arcsec)	Member	Commen
	(2000.0)													
001	8 35	38.59	-53 13	15.5	—	12.804	0.977	—	11.351	10.405	10.183	0.03	NM	RED
002	8 35	44.88	-53 25	55.6	—	17.157	2.260	—	—	—	—	—	MEM?	Faint
003	8 35	51.96	-53 18	25.8	—	13.665	1.299	—	12.474	11.836	11.592	0.08	MEM	
004	8 35	57.90	-53 22	17.6	—	17.554	2.433	—	—	—	—	—	MEM?	Faint
005	8 36	4.08	-53 29	25.0	—	16.417	1.832	—	14.782	14.178	13.980	0.04	MEM?	
005	8 36	4.09	-53 29	25.0	—	16.425	1.779	—	14.782	14.178	13.980	0.13	MEM?	RII
006	8 36	7.21	-53 25	41.2	—	16.879	2.171	—	—	—	—	—	NM?	NM-IR
007	8 36	40.36	-53 21	30.0	—	16.518	1.983	—	14.625	13.996	13.791	0.11	MEM	
008	8 36	40.72	-52 44	30.0	19.29	16.306	2.037	—	16.372	15.411	15.179	0.16	NM	VRRI
009	8 36	42.73	-53 7	58.4	18.33	15.370	1.539	0.56	13.946	13.311	13.028	0.13	MEM?	RII
010	8 36	44.44	-53 19	36.5	—	12.348	0.994	—	—	—	—	—	NM?	NM-IR
011	8 36	44.71	-53 19	33.9	—	12.348	0.995	—	10.896	10.040	9.691	0.09	NM	RED
012	8 36	45.71	-53 11	32.6	18.78	15.553	1.672	0.63	13.935	13.251	12.992	0.51	MEM	
013	8 36	46.24	-53 21	39.8	—	13.985	1.620	—	12.486	11.954	11.664	0.22	MEM	
014	8 36	56.03	-53 23	57.3	—	16.682	2.077	—	—	—	—	—	NM?	NM-IR
015	8 37	2.09	-53 21	39.6	—	16.264	1.986	—	15.458	14.913	14.757	1.95	NM	RIIK
016	8 37	8.70	-53 15	0.5	—	12.133	0.925	—	10.840	10.163	9.866	0.08	MEM	
017	8 37	11.45	-52 36	35.6	19.30	15.989	1.752	—	14.461	13.860	13.587	0.24	MEM	SPEC+
018	8 37	11.85	-53 26	3.8	—	14.319	1.406	—	13.115	12.542	12.352	0.10	MEM?	JKK
019	8 37	11.90	-52 59	16.0	—	18.464	2.472	—	—	—	—	0.16	MEM?	Faint
020	8 37	12.07	-53 20	46.4	—	12.956	0.999	—	11.484	10.592	10.371	0.13	NM	RED
021	8 37	12.96	-53 21	29.9	—	12.149	0.795	—	10.993	10.408	10.213	0.07	MEM	
022	8 37	13.53	-53 20	3.2	—	13.013	1.474	—	11.145	10.156	9.782	0.07	NM	RED
023	8 37	14.90	-53 20	21.2	—	12.248	0.886	—	—	—	—	—	NM?	NM-IR
024	8 37	15.23	-53 20	18.3	—	12.248	0.888	—	11.267	10.544	10.427	0.10	MEM	
025	8 37	15.22	-53 24	13.0	18.29	15.172	1.760	0.60	13.640	12.990	12.719	0.08	MEM	
025	8 37	15.23	-53 24	13.1	18.29	15.136	1.783	0.60	13.640	12.990	12.719	0.19	MEM	
026	8 37	18.19	-52 55	56.9	—	16.352	2.001	—	14.507	13.880	13.492	0.08	MEM	
027	8 37	19.82	-52 42	6.0	—	12.562	1.144	—	10.848	9.871	9.600	0.08	NM	RED
028	8 37	22.26	-52 39	3.9	18.56	15.454	1.671	—	13.932	13.356	13.165	0.12	MEM?	JKK
029	8 37	24.37	-53 16	49.2	—	16.542	1.991	—	14.694	14.085	13.738	0.25	MEM	
030	8 37	27.69	-52 51	10.8	—	15.863	1.935	—	13.937	13.318	12.994	0.04	MEM	
031	8 37	32.81	-53 3	33.6	18.24	15.336	1.699	0.53	13.899	13.398	13.080	0.08	MEM	
031	8 37	32.81	-53 3	33.6	18.24	15.336	1.699	0.53	13.899	13.398	13.080	0.08	MEM	
032	8 37	34.99	-53 29	24.9	19.04	15.366	1.966	0.74	13.497	12.905	12.648	0.07	MEM	
032	8 37	34.99	-53 29	24.9	19.04	15.366	1.966	0.74	13.497	12.905	12.648	0.07	MEM	
033	8 37	43.07	-53 14	14.2	—	20.383	2.541	—	—	—	—	—	MEM?	Faint
034	8 37	47.77	-52 39	38.5	—	12.488	0.864	—	11.225	10.524	10.308	0.32	MEM	
035	8 37	47.74	-53 8	22.3	19.01	15.760	1.732	0.59	14.276	13.613	13.376	0.20	MEM	
035	8 37	47.76	-53 8	22.1	19.01	15.747	1.784	0.59	14.276	13.613	13.376	0.06	MEM	
036	8 37	49.11	-52 46	28.6	—	12.418	1.017	—	10.858	9.917	9.679	0.09	NM	RED
037	8 37	58.91	-52 46	15.0	—	13.122	1.083	—	11.463	10.490	10.186	0.15	NM	RED
038	8 37	59.20	-53 21	55.4	19.90	16.291	1.910	0.71	14.455	13.869	13.643	0.10	MEM	SPEC+
039	8 38	0.19	-52 42	13.4	—	15.230	1.528	—	13.885	13.097	13.002	0.18	MEM	
040	8 38	0.48	-53 27	24.9	21.60	17.456	2.120	0.84	15.603	14.909	14.486	0.10	NM	SPEC-

Table 2: IC2391 candidate members.

CTIO	ALPHA		DELTA		V	$I_C$	$(R-I)_C$	$(I-Z)$	J	H	$K_s$	dist (arcsec)	Member	Commer
	(2000.0)													
041	8 38 11.88	-52 22 51.3	20.46	16.554	1.923	0.79	14.630	14.088	13.741	0.29	MEM	SPEC+		
042	8 38 12.33	-52 44 41.4	19.09	16.067	1.698	-	14.380	13.818	13.492	0.18	MEM?	VVI		
042	8 38 12.34	-52 44 41.5	19.09	15.974	1.706	-	14.380	13.818	13.492	0.26	MEM?			
043	8 38 14.19	-52 52 12.0	-	12.485	1.032	-	10.912	9.983	9.752	0.21	NM	RED		
043	8 38 14.19	-52 52 12.0	-	12.485	1.032	-	10.912	9.983	9.752	0.21	NM	RED		
044	8 38 14.41	-52 45 0.1	-	12.301	0.891	-	10.915	10.174	9.938	0.12	MEM			
044	8 38 14.41	-52 45 0.1	-	12.301	0.891	-	10.915	10.174	9.938	0.12	MEM			
045	8 38 19.97	-52 49 29.3	-	13.240	1.098	-	11.518	10.517	10.251	0.06	NM	RED		
045	8 38 19.97	-52 49 29.3	-	13.240	1.098	-	11.518	10.517	10.251	0.06	NM	RED		
046	8 38 25.09	-53 19 10.9	18.92	15.958	1.697	0.62	14.420	13.803	13.435	0.14	MEM?	VVI		
046	8 38 25.09	-53 19 10.9	18.92	15.958	1.697	0.62	14.420	13.803	13.435	0.14	MEM?	VVI		
047	8 38 25.32	-53 5 35.7	19.21	15.995	1.708	0.57	14.614	13.972	13.720	0.95	MEM?	IIK		
047	8 38 25.32	-53 5 35.7	19.21	15.995	1.708	0.57	14.614	13.972	13.720	0.95	MEM?	IIK		
048	8 38 26.72	-53 10 7.4	18.72	15.753	1.676	0.52	14.362	13.824	13.521	0.11	MEM?	IIK		
048	8 38 26.75	-53 10 7.3	18.72	15.767	1.642	0.52	14.362	13.824	13.521	0.23	MEM?	IIK		
049	8 38 27.15	-53 25 10.4	19.05	15.566	1.944	-	13.928	13.336	13.002	0.24	MEM			
050	8 38 28.24	-52 40 57.1	-	20.944	2.494	-	-	-	-	0.00	MEM?	Faint		
051	8 38 34.31	-52 50 49.4	-	17.573	2.510	-	-	-	-	-	MEM?	Faint		
052	8 38 34.93	-53 4 44.5	-	17.505	2.271	0.96	-	-	-	-	MEM?	Faint		
053	8 38 35.13	-53 0 52.7	-	18.999	2.415	-	-	-	-	-	MEM?	Faint		
054	8 38 36.09	-53 25 52.0	-	20.629	2.542	-	-	-	-	-	MEM?	Faint		
055	8 38 36.98	-52 52 42.6	-	15.341	1.741	-	13.781	13.176	12.886	0.19	MEM			
056	8 38 38.79	-53 7 57.5	-	16.711	1.837	-	15.314	14.631	14.365	0.14	MEM?	IIK		
057	8 38 42.25	-52 30 37.1	19.08	15.471	1.972	0.64	13.930	13.315	13.018	0.17	MEM			
058	8 38 42.34	-53 29 31.3	-	19.919	2.661	-	-	-	-	-	MEM?	Faint		
059	8 38 44.02	-53 22 50.9	19.47	16.050	1.819	0.63	14.460	13.757	13.526	0.17	MEM	SPEC+		
060	8 38 45.91	-52 51 6.1	-	12.302	0.894	-	10.926	10.064	9.843	0.17	NM	RED		
061	8 38 47.06	-52 14 56.3	-	17.309	2.141	-	15.274	14.677	14.206	0.19	MEM	SPEC+		
062	8 38 47.29	-52 44 32.8	20.84	16.782	2.139	-	14.954	14.389	13.989	0.18	MEM	SPEC+		
062	8 38 47.30	-52 44 32.7	20.84	16.765	2.000	-	14.954	14.389	13.989	0.20	MEM	SPEC+		
062	8 38 47.31	-52 44 32.3	20.84	16.754	2.047	-	14.954	14.389	13.989	0.41	MEM	SPEC+		
063	8 38 49.59	-52 36 31.0	-	20.841	2.522	-	-	-	-	0.47	MEM?	Faint		
064	8 38 51.88	-52 50 8.7	-	12.492	0.997	-	11.002	10.099	9.831	0.26	NM	RED		
065	8 38 53.30	-52 47 48.8	-	12.360	0.915	-	10.986	10.188	9.926	0.24	NM	RED		
066	8 38 54.95	-52 35 23.0	19.40	16.007	1.750	-	14.681	14.073	13.849	0.32	MEM?	IIK		
067	8 38 56.19	-52 51 38.0	-	17.111	2.285	-	-	-	-	-	MEM?	Faint		
068	8 39 2.00	-52 52 55.3	-	18.611	2.410	-	-	-	-	0.41	MEM?	Faint		
068	8 39 2.00	-52 52 55.3	-	18.611	2.410	-	-	-	-	0.41	MEM?	Faint		
069	8 39 5.76	-52 23 13.6	-	15.561	1.632	0.59	13.942	13.307	13.019	0.27	MEM			
070	8 39 8.95	-52 37 41.8	20.75	17.052	1.916	-	15.525	14.903	14.563	0.25	MEM?	IIK		
070	8 39 8.95	-52 37 41.8	20.75	17.052	1.916	-	15.525	14.903	14.563	0.25	MEM?	IIK		
071	8 39 10.68	-52 30 11.9	-	18.167	2.270	-	-	-	-	0.40	MEM?	Faint		
072	8 39 27.48	-53 34 52.3	18.43	15.718	1.722	-	14.011	13.378	13.161	0.55	NM	VRRI		
073	8 39 32.05	-53 28 12.6	-	20.322	2.620	-	-	-	-	-	MEM?	Faint		
074	8 39 40.59	-53 6 7.6	-	15.876	1.786	-	14.191	13.526	13.278	0.34	MEM			
075	8 39 41.44	-53 4 3.5	17.80	14.996	1.520	0.52	13.702	13.027	12.800	0.32	MEM?			
075	8 39 41.51	-53 4 3.6	17.80	15.076	1.495	0.52	13.702	13.027	12.800	0.95	MEM?	VVI		
076	8 39 48.44	-53 13 58.4	18.47	15.278	1.681	0.61	13.664	13.045	12.745	0.17	MEM			
076	8 39 48.44	-53 13 58.4	18.47	15.278	1.681	0.61	13.664	13.045	12.745	0.17	MEM			
077	8 40 9.53	-53 37 49.6	20.04	16.308	1.929	-	14.543	13.962	13.632	0.24	MEM	SPEC+		
078	8 40 10.05	-52 35 11.9	18.59	15.060	1.928	0.66	13.338	12.738	12.463	0.55	MEM			
079	8 40 10.84	-52 37 15.5	-	20.302	2.733	-	-	-	-	-	MEM?	Faint		
080	8 40 14.57	-52 42 24.7	-	19.659	2.549	-	-	-	-	-	MEM?	Faint		

Table 2: IC2391 candidate members.

CTIO	ALPHA		DELTA		V	$I_C$	$(R-I)_C$	$(I-Z)$	J	H	$K_s$	dist (arcsec)	Member	Commen
	(2000.0)													
081	8 40	14.76	-53 27	36.4	20.38	16.465	2.079	—	14.370	13.745	13.394	0.22	MEM	SPEC+
082	8 40	15.17	-52 40	24.7	20.93	16.625	2.173	0.89	14.558	13.889	13.476	0.19	MEM	
083	8 40	16.07	-53 25	47.8	18.85	15.565	1.799	—	13.906	13.272	12.933	0.36	MEM	
084	8 40	33.36	-52 34	39.9	—	20.847	2.568	—	—	—	—	0.19	MEM?	Faint
085	8 40	38.18	-53 7	56.8	—	20.255	2.712	—	—	—	—	—	MEM?	Faint
086	8 40	39.34	-52 47	25.8	—	19.698	2.524	—	—	—	—	—	MEM?	Faint
087	8 40	42.91	-53 9	18.9	—	20.240	2.503	—	—	—	—	0.16	MEM?	Faint
088	8 40	44.37	-53 7	0.0	—	17.622	2.111	0.93	15.229	14.650	14.579	0.38	MEM?	JKK
089	8 40	46.81	-53 13	52.0	—	19.971	2.726	—	—	—	—	—	MEM?	Faint
090	8 40	47.47	-53 7	8.1	—	20.213	2.488	—	—	—	—	—	MEM?	Faint
091	8 40	53.00	-52 23	0.4	—	15.842	1.765	—	14.082	13.460	13.174	0.36	MEM	
092	8 40	54.93	-52 47	50.2	—	20.555	2.520	—	—	—	—	—	MEM?	Faint
093	8 40	55.19	-52 34	50.2	18.86	15.347	1.950	0.70	13.657	13.020	12.686	0.25	MEM	
094	8 41	2.88	-52 32	4.6	18.27	15.307	1.736	0.56	13.942	13.316	13.014	0.86	NM	SPEC-
095	8 41	6.93	-53 5	19.5	—	20.261	2.765	—	—	—	—	0.01	MEM?	Faint
096	8 41	12.37	-53 9	10.3	—	16.144	1.912	—	14.344	13.818	13.404	0.12	MEM	SPEC+
096	8 41	12.37	-53 9	10.3	19.75	16.144	1.912	0.70	14.344	13.818	13.404	0.12	MEM	SPEC+
097	8 41	25.99	-53 26	34.8	—	15.087	1.751	0.61	13.456	12.761	12.541	0.03	MEM	
098	8 41	29.17	-53 16	22.2	18.87	15.593	1.797	0.63	13.988	13.333	13.060	0.10	MEM	
099	8 41	32.63	-52 41	5.6	19.35	16.206	1.790	—	14.646	14.053	13.820	0.05	MEM?	VVI
099	8 41	32.63	-52 41	5.7	19.35	16.221	1.694	—	14.646	14.053	13.820	0.15	MEM?	VVI
100	8 41	35.96	-53 9	27.1	18.46	15.076	1.796	0.62	13.488	12.883	12.600	0.23	MEM	
101	8 41	39.24	-53 4	28.7	—	19.995	2.733	—	—	—	—	—	MEM?	Faint
102	8 41	41.48	-53 27	50.7	—	20.130	2.523	—	—	—	—	—	MEM?	Faint
103	8 41	43.96	-53 14	7.0	17.74	14.596	1.723	0.60	13.086	12.463	12.152	0.16	MEM	
104	8 41	51.92	-53 29	11.5	—	20.318	2.740	—	—	—	—	—	MEM?	Faint
105	8 41	54.01	-53 5	4.8	—	20.241	2.529	—	—	—	—	2.78	MEM?	Faint
106	8 41	58.93	-53 12	36.3	—	16.454	1.983	—	14.655	13.997	13.676	0.61	MEM	SPEC+
106	8 41	58.93	-53 12	36.3	—	16.454	1.983	—	14.655	13.997	13.676	0.61	MEM	SPEC+
106	8 41	58.99	-53 12	36.9	—	16.561	2.007	—	14.618	14.034	13.674	0.13	MEM	SPEC+
106	8 41	58.99	-53 12	36.9	—	16.561	2.007	—	14.618	14.034	13.674	0.13	MEM	SPEC+
107	8 42	4.65	-52 32	26.5	19.11	15.913	1.651	—	14.539	13.815	13.603	0.02	MEM?	RII
108	8 42	4.91	-52 53	54.1	—	13.315	1.413	—	12.075	11.392	11.140	0.19	MEM	
109	8 42	8.79	-52 44	49.7	—	12.652	1.254	—	11.451	10.792	10.551	0.07	MEM	
110	8 42	11.66	-52 52	1.0	—	18.036	2.391	—	—	—	—	—	MEM?	Faint
111	8 42	12.31	-52 43	14.5	—	17.493	2.380	—	—	—	—	—	MEM?	Faint
112	8 42	13.58	-52 47	59.1	—	12.308	0.982	—	10.878	9.982	9.789	0.11	NM	RED
113	8 42	18.71	-52 39	40.0	21.90	17.282	2.135	—	15.083	14.377	14.030	0.20	MEM	SPEC+
113	8 42	18.72	-52 39	40.1	21.90	17.365	2.281	—	15.083	14.377	14.030	0.27	MEM	SPEC+
114	8 42	21.56	-52 53	38.9	—	12.506	0.849	—	11.329	10.566	10.367	0.15	MEM	
115	8 42	21.99	-52 47	57.1	—	16.519	1.984	—	—	—	—	—	NM?	NM-IR
116	8 42	26.46	-52 47	7.0	—	17.799	2.305	—	—	—	—	—	MEM?	Faint
117	8 42	28.14	-52 43	19.7	—	17.691	2.653	—	—	—	—	—	MEM?	Faint
118	8 42	29.69	-53 3	33.2	—	19.888	2.595	—	—	—	—	—	MEM?	Faint
119	8 42	30.01	-52 47	0.4	—	12.931	1.097	—	11.266	10.251	9.982	0.09	NM	RED
120	8 42	32.88	-52 47	26.2	—	13.306	1.496	—	11.158	9.955	9.524	0.05	NM	RED

Table 2: IC2391 candidate members.

CTIO	ALPHA	DELTA	V	$I_C$	$(R-I)_C$	$(I-Z)$	J	H	$K_s$	dist	Member	Commen
	(2000.0)					CTIO				(arcsec)		
121	8 42 33.53	-52 44 27.4	—	17.500	2.337	—	—	—	—	1.40	MEM?	Faint
122	8 42 33.68	-52 53 54.8	—	12.049	0.946	—	10.682	9.830	9.575	0.05	NM	RED
123	8 42 43.59	-52 50 57.5	—	16.404	2.239	—	—	—	—	—	NM?	NM-IR
124	8 42 45.80	-52 50 6.5	—	17.363	2.043	—	15.205	14.579	14.380	0.16	MEM?	RII
124	8 42 45.80	-52 50 6.5	—	17.363	2.043	—	15.205	14.579	14.380	0.16	MEM?	RII
125	8 42 46.35	-52 46 52.8	—	12.985	1.000	—	11.424	10.607	10.314	0.09	NM	RED
125	8 42 46.35	-52 46 52.8	—	12.985	1.000	—	11.424	10.607	10.314	0.09	NM	RED
126	8 42 49.05	-52 52 15.9	—	14.389	1.802	—	12.741	12.105	11.880	0.15	MEM	
127	8 42 53.31	-52 48 55.6	—	16.071	1.686	—	14.484	13.812	13.648	0.36	MEM?	RII
128	8 42 54.79	-52 46 38.1	—	13.124	1.054	—	—	—	—	—	NM?	NM-IR
129	8 42 55.44	-52 43 11.7	—	13.105	1.070	—	11.519	10.635	10.423	0.31	NM	RED
130	8 42 58.21	-52 49 46.2	—	17.227	2.031	—	15.402	14.772	14.462	0.36	MEM	
131	8 43 3.51	-53 26 57.3	—	15.167	1.710	—	13.685	13.067	12.764	0.24	MEM	
132	8 43 5.60	-53 31 36.2	—	17.454	2.261	—	15.441	14.821	14.278	0.25	MEM	
132	8 43 5.62	-53 31 36.2	—	17.440	2.113	—	15.441	14.821	14.278	0.15	MEM	
133	8 43 10.60	-52 50 13.6	—	13.063	1.325	—	11.773	11.092	10.854	0.13	MEM	
134	8 43 12.87	-52 43 31.6	—	12.891	1.192	—	11.135	10.144	9.792	0.15	NM	RED
135	8 43 13.02	-53 29 8.5	—	14.377	1.825	—	12.775	12.150	11.871	0.25	MEM	
136	8 43 15.14	-52 58 23.0	19.72	15.868	1.978	0.71	14.134	13.482	13.129	0.22	MEM	SPEC+
137	8 43 15.25	-53 29 9.5	—	17.833	2.363	—	—	—	—	—	MEM?	Faint
138	8 43 15.39	-52 51 23.2	—	12.377	0.852	—	11.121	10.430	10.251	0.12	MEM	
139	8 43 15.51	-52 38 49.5	17.80	14.721	1.560	0.63	12.885	12.244	11.937	0.20	MEM	
140	8 43 16.58	-52 40 59.7	—	17.690	2.172	—	—	—	—	2.04	MEM?	Faint
141	8 43 18.17	-52 48 41.9	—	17.084	2.045	—	15.794	15.130	14.735	2.16	MEM?	IJK
142	8 43 18.82	-52 53 15.3	—	18.000	2.453	—	16.661	15.871	15.587	2.96	NM?	RIJK
143	8 43 19.85	-53 31 30.6	—	12.206	0.767	—	11.098	10.344	10.133	0.07	MEM	
143	8 43 19.85	-53 31 30.6	—	12.206	0.767	—	11.098	10.344	10.133	0.07	MEM	
144	8 43 23.76	-53 14 16.2	—	16.943	2.032	—	15.059	14.386	13.962	0.16	MEM	
144	8 43 23.76	-53 14 16.2	—	16.943	2.032	—	15.059	14.386	13.962	0.16	MEM	
145	8 43 23.66	-53 14 16.8	—	16.936	2.135	—	15.059	14.386	13.962	1.11	MEM	SPEC+
146	8 43 29.90	-53 30 20.0	—	17.117	2.262	—	16.078	15.327	15.182	2.30	NM?	RIJK
146	8 43 29.90	-53 30 20.0	—	17.117	2.262	—	16.078	15.327	15.182	2.30	NM?	RIJK
147	8 43 34.33	-52 43 55.7	—	17.481	2.475	—	—	—	—	—	MEM?	Faint
148	8 43 35.21	-52 41 13.7	—	12.307	0.856	—	11.135	10.430	10.230	0.17	MEM	
149	8 43 37.12	-52 47 6.2	—	15.287	1.689	—	13.814	13.214	12.906	0.01	MEM	
150	8 43 37.16	-52 45 52.2	—	13.220	1.119	—	11.588	10.541	10.278	0.06	NM	RED
151	8 43 37.32	-52 48 57.9	—	16.270	2.194	—	15.386	14.800	14.716	2.15	NM	RIJK
152	8 43 38.42	-52 50 55.4	18.11	14.891	1.781	0.57	13.337	12.714	12.452	0.24	MEM	SPEC+
152	8 43 38.43	-52 50 55.3	18.11	14.870	1.785	0.57	13.337	12.714	12.452	0.16	MEM	SPEC+
153	8 43 38.93	-53 21 55.8	—	12.332	0.846	—	11.112	10.219	10.033	0.06	NM	RED
154	8 43 39.28	-52 52 20.3	—	17.569	2.367	—	—	—	—	0.59	MEM?	Faint
155	8 43 40.12	-52 46 30.9	—	16.763	2.295	—	—	—	—	—	NM?	NM-IR
156	8 43 40.22	-53 29 57.6	—	13.016	1.026	—	11.497	10.516	10.322	0.08	NM	RED
157	8 43 42.14	-53 19 50.1	—	13.101	1.271	—	11.546	10.579	10.258	0.02	NM	RED
158	8 43 48.11	-53 32 57.0	—	15.910	1.675	—	14.015	13.401	13.069	0.14	MEM?	RII
159	8 43 58.74	-53 30 34.1	—	17.294	2.315	—	—	—	—	—	MEM?	Faint
160	8 44 2.09	-52 44 10.6	21.05	17.161	2.159	0.84	15.115	14.468	14.103	0.16	MEM?	VVI
160	8 44 2.10	-52 44 10.9	21.05	17.141	2.020	0.84	15.115	14.468	14.103	0.13	MEM?	VVI

Table 2: IC2391 candidate members.

CTIO	ALPHA	DELTA	V	$I_C$	$(R-I)_C$	$(I-Z)$	J	H	$K_s$	dist	Member	Commer
	(2000.0)					<i>CTIO</i>				(arcsec)		
161	8 44 2.95	-53 26 32.7	—	12.315	0.911	—	10.973	10.064	9.830	0.20	NM	RED
162	8 44 6.38	-53 32 28.8	—	12.223	0.963	—	10.742	9.862	9.640	0.14	NM	RED
163	8 44 7.59	-53 29 56.3	—	12.100	0.813	—	10.848	10.103	9.891	0.05	MEM	
164	8 44 14.99	-53 21 52.9	—	12.022	0.726	—	10.919	10.326	10.118	0.00	MEM	
165	8 44 17.04	-53 13 42.9	—	20.174	2.508	—	—	—	—	—	MEM?	Faint
166	8 44 24.18	-53 1 54.4	—	12.392	1.133	—	10.831	9.816	9.548	0.24	NM	RED
167	8 44 26.16	-52 35 41.4	19.41	16.341	1.700	—	14.953	14.263	14.170	0.16	MEM?	JJK
168	8 44 27.31	-52 49 39.2	—	12.818	1.060	—	11.303	10.394	10.120	0.29	NM	RED
169	8 44 27.76	-52 56 47.6	—	16.042	1.885	—	15.262	14.780	14.513	1.96	NM	RIIK
170	8 44 28.31	-53 23 24.7	—	17.592	2.387	—	—	—	—	—	MEM?	Faint
171	8 44 29.78	-53 26 37.9	—	16.386	1.742	—	—	—	—	—	NM?	NM-IR
172	8 44 30.10	-53 26 36.3	—	13.923	1.356	—	12.755	12.037	11.797	0.02	MEM	
173	8 44 31.73	-53 25 54.5	—	12.557	0.861	—	11.256	10.491	10.204	0.11	NM	RED
174	8 44 34.21	-53 8 32.1	—	16.978	2.275	—	14.522	13.908	13.580	0.08	MEM	
175	8 44 37.64	-53 32 18.0	—	12.144	0.743	—	11.141	10.531	10.372	2.91	MEM	
176	8 44 39.60	-53 2 46.5	—	17.460	2.436	—	—	—	—	—	MEM?	Faint
177	8 44 40.37	-52 44 2.0	—	16.826	1.843	—	15.219	14.674	14.402	0.13	MEM?	IJK
178	8 44 43.37	-53 3 25.9	—	19.890	2.592	—	—	—	—	0.99	MEM?	Faint
179	8 44 44.63	-52 42 15.2	—	17.497	2.096	—	15.705	15.232	14.749	0.17	MEM	
180	8 44 47.97	-52 50 49.1	—	12.083	1.082	—	10.483	9.492	9.197	0.18	NM	RED
180	8 44 47.97	-52 50 49.1	—	12.083	1.082	—	10.483	9.492	9.197	0.18	NM	RED
181	8 44 49.88	-52 55 30.4	—	17.599	2.591	—	—	—	—	—	MEM?	Faint
182	8 44 50.00	-52 55 16.1	—	16.097	1.670	—	14.611	13.858	13.656	0.09	MEM?	RII
182	8 44 50.00	-52 55 16.1	—	16.097	1.670	—	14.611	13.858	13.656	0.09	MEM?	RII
183	8 45 2.60	-53 14 33.5	—	17.050	1.927	—	15.161	14.627	14.283	0.15	MEM?	RII
184	8 45 2.63	-52 54 2.6	—	12.660	0.898	—	11.212	10.355	10.168	0.19	NM	RED
185	8 45 14.83	-52 51 37.3	—	16.391	1.796	—	15.484	15.127	14.732	1.80	NM	RIIK
186	8 45 16.42	-52 49 35.8	—	12.114	0.833	—	10.971	10.306	10.136	0.37	MEM	
187	8 45 17.58	-52 51 40.7	—	18.107	2.231	—	—	—	—	—	MEM?	Faint
188	8 45 18.80	-52 59 25.8	—	15.367	1.754	—	13.775	13.214	12.875	0.24	MEM	
189	8 45 22.62	-52 50 36.6	—	16.543	2.205	—	15.047	14.329	14.027	1.65	MEM	
190	8 45 24.69	-53 1 22.7	—	14.872	1.648	—	13.383	12.831	12.472	0.13	MEM	

Table 2: IC2391 candidate members.

CTIO	ALPHA	DELTA	V	I <sub>C</sub>	(R-I) <sub>C</sub>	(I-Z) CTIO	J	H	K <sub>s</sub>	dist (arcsec)	Member	Commen
	(2000.0)											
191	8 45 30.19	-53 11 59.9	–	20.218	2.507	–	–	–	–	–	MEM?	Faint
192	8 45 42.58	-52 59 28.7	–	16.286	1.970	–	14.460	13.853	13.527	0.22	MEM	
192	8 45 42.58	-52 59 28.7	–	16.286	1.970	–	14.460	13.853	13.527	0.22	MEM	
192	8 45 42.58	-52 59 28.7	–	16.286	1.970	–	14.460	13.853	13.527	0.22	MEM	
193	8 45 44.12	-52 57 0.8	–	16.394	1.782	–	14.717	14.045	13.741	0.95	MEM?	RII
194	8 45 44.26	-53 0 54.1	–	16.928	1.885	–	–	–	–	0.83	NM?	NM-IR
195	8 45 45.59	-53 12 37.8	–	16.353	1.869	–	14.566	13.986	13.611	0.14	MEM	
195	8 45 45.66	-53 12 37.4	–	16.241	1.941	–	14.566	13.986	13.611	0.55	MEM	
196	8 45 52.60	-52 43 32.7	–	17.978	2.254	–	–	–	–	0.77	MEM?	Faint
197	8 45 57.67	-52 52 56.6	–	12.876	1.187	–	11.312	10.292	9.959	1.00	NM	RED
198	8 45 57.85	-52 53 2.8	–	12.891	0.995	–	11.493	10.629	10.335	0.97	NM	RED
199	8 45 58.45	-52 58 53.3	–	17.420	2.162	–	–	–	–	2.44	MEM?	Faint
200	8 45 59.82	-52 54 38.0	–	12.049	0.837	–	10.855	10.099	9.885	1.06	MEM	
201	8 46 0.07	-52 54 35.3	–	12.049	0.837	–	10.855	10.099	9.885	2.66	MEM	
202	8 46 26.27	-53 1 53.4	–	16.391	2.057	–	14.472	13.962	13.551	0.19	MEM	
203	8 46 42.17	-52 44 13.4	19.25	15.980	1.688	–	14.556	13.915	13.683	0.06	MEM?	IJK
204	8 46 42.43	-53 13 27.2	–	20.741	2.577	–	–	–	–	2.25	MEM?	Faint
205	8 47 3.46	-52 46 52.3	20.21	16.211	2.065	–	14.217	13.744	13.350	0.11	MEM	SPEC+
205	8 47 3.46	-52 46 52.3	20.21	16.211	2.065	–	14.217	13.744	13.350	0.11	MEM	SPEC+
206	8 40 40.84	-53 13 31.8	–	15.658	1.730	–	13.697	13.132	12.785	0.24	MEM	SPEC+

SPEC+ = Probable member based on spectroscopy

SPEC– = Probable member based on spectroscopy

RED = high reddening

VRR1 = Probable non-member based on the (V-R),(R-I) diagram

RIIK = Probable non-member based on the (R-I),(I-K) diagram

Faint = Too faint to be detected by 2MASS

NM-IR = No 2MASS data, but bright.

JKK = Possible member based on the K,(J-K) diagram

IJK = Possible member based on the I,(I-K) diagram

VVI = Possible member based on the V,(V-I) diagram

RII = Possible member based on the I,(R-I) diagram